Journal of Industrial and Management Optimization

https://www.aimspress.com/journal/jimo

JIMO, 22(12): 6593–6637.
DOI:10.3934/jimo.2026221
Received: 21 September 2026
Revised: 04 November 2026
Accepted: 10 November 2026
Published: 17 November 2026

Research article

Embedding disruption-generated delay losses to co-optimize greenness, timeliness, and resilience under 4PL-driven coordination for winner determination in liner shipping procurement auctions

Mingkun Yu[1], Liyan Wang[1,*], Mingqiang Yin[1,2,3,*], Linlin Kong[1], Guihua Bo[1] and Xiaohu Qian[4]

[1] School of Information and Control Engineering, Liaoning Petrochemical University, Fushun, Liaoning 113001, China
[2] Chongqing Rongguan Science Technologies Co., Ltd., Chongqing 400039, China
[3] Chongqing Jiaotong University, Chongqing 400074, China
[4] Research Institute of Business Analytics and Supply Chain Management, College of Management, Shenzhen University, Shenzhen 518060, China

* **Correspondence:** Emails: wangliyan2015atlnpu@lnpu.edu.cn; yinmingqiang2387@sina.com.

Abstract: Disruptions in liner shipping service procurement (LSSP) reduce available transportation capacity and cause delays, additional costs, and sustainability challenges. Existing studies of the winner determination problem (WDP) emphasize procurement cost and provider selection, with limited integration of disruption-induced third-party logistics (3PL) capacity losses, carbon emission control, soft-time-window deviation costs, and coordinated resilience strategies. This study investigates a WDP for LSSP auctions under disruption risk from a fourth-party logistics (4PL) perspective by integrating greenness, timeliness, and resilience. A hybrid strategy combining multilevel fortification, capacity reservation, and emergency outsourcing mitigates capacity losses, and soft time windows quantify earliness and tardiness penalties. A two-stage stochastic winner determination model with a carbon emission cap is formulated and reformulated as a mixed-integer linear programming model. A hybrid algorithm integrating scenario reduction with scenario-sorting-based dual decomposition and Lagrangian relaxation (SR-SSDDLR) is developed for large-scale disruption scenarios. Experiments based on African container shipping data confirm the model's computational efficiency and stability. Sensitivity analyses and strategy comparisons indicate that protective investment and soft time-window settings jointly shape procurement costs and hybrid resilience strategy configuration under capacity losses and a carbon emission cap. The findings guide 4PLs in coordinating multiple 3PL resources and developing cost-effective and sustainable LSSP plans under disruptions.

Keywords: liner shipping service procurement; winner determination; greenness; soft time windows; hybrid resilience strategy
Mathematics Subject Classification: 90B06, 90C15, 90C11

1. Introduction

Maritime transport is fundamental to international trade and the operation of global supply chains, as more than 80% of international merchandise trade by volume is carried by sea [1]. With increasing specialization and outsourcing in maritime logistics, liner shipping services are commonly procured from third-party logistics (3PL) providers. Given the differences among 3PLs in route coverage, available capacity, bids, and service levels, a key decision problem for firms is how suitable providers should be selected and the corresponding resources integrated for cross-regional transportation task allocation. The rise of fourth-party logistics (4PL) has enabled closer integration of the service resources of multiple 3PLs and coordination of liner shipping service procurement (LSSP). As a supply chain integrator and procurement decision-maker, a 4PL aggregates shipper demand and integrates information on the transportation resources, service capabilities, and bids of multiple 3PLs to establish an organizational framework for joint decisions on 3PL selection and transportation task allocation. Tao et al. [2] showed that a 4PL can reduce carbon emissions by coordinating transportation planning and integrating the complementary service capabilities and logistics resources of multiple 3PLs. Qian et al. [3] showed that transportation service procurement (TSP) auctions organized by a 4PL can facilitate 3PL resource integration and enhance the flexibility and sustainability of transportation services. Zhou et al. [4] emphasized that winner determination can be optimized through 4PL-coordinated resource integration to support sustainable supply chain operations and improve transport timeliness. Optimizing winner determination in 4PL-led TSP auctions can coordinate resources across multiple 3PLs and provide a new approach to resource allocation among multiple participants in cross-border liner shipping while supporting efficient and sustainable service procurement.

In recent years, critical maritime routes have been frequently disrupted by geopolitical conflicts, accidents, port congestion, and extreme weather, further heightening uncertainty in LSSP. In 2021, the grounding of the container ship *Ever Given* caused a blockage of the Suez Canal for nearly a week; the resulting vessel diversions increased carbon emissions and associated environmental costs [5]. Since late 2023, numerous vessels have had to reroute around the Cape of Good Hope due to the Red Sea security crisis, leading to longer voyages and changes to liner service schedules [6]. Following the escalation of military tensions in the Middle East in late February 2026, vessel traffic through the Strait of Hormuz declined sharply [7]. Despite differences in their causes, duration, and scope, these events collectively indicate that disruptions along key maritime routes can reduce available 3PL capacity, lengthen transit times and sailing distances, disrupt liner schedules, increase fuel consumption and carbon emissions, and raise emergency transportation and fulfillment costs, thereby undermining the execution of established procurement plans. To quantify the costs caused by deviations of task completion times from customer-preferred time windows, soft time windows with earliness and tardiness penalties are included in the winner determination problem (WDP). Salani and Battarra [8] showed that moderate deviations from specified delivery windows are often acceptable in practice, and time window violation costs can be used to balance transport efficiency and service levels. El Noshokaty [9] further applied soft time windows to stochastic shipping scheduling and showed that the inclusion of earliness and tardiness costs provides greater flexibility in vessel routing and schedule adjustments than models without these penalties. Capacity losses affect whether transportation demand can be met by the winning bids, and task completion times and emission

factors influence the associated time window penalties and transportation emissions. Capacity losses, task completion times, and emission factors must therefore be considered when winning bids are selected, transportation volumes are allocated, and resilience measures are determined to meet demand and control total procurement cost.

In this study, a WDP for LSSP auctions under disruption risk is investigated from a 4PL perspective. Soft time windows are introduced to quantify earliness and tardiness penalties, and a carbon emission cap is imposed to control transportation emissions. A hybrid resilience strategy comprising multilevel fortification, capacity reservation, and emergency outsourcing is incorporated into the WDP to mitigate disruption-induced capacity losses. Discrete scenarios are used to represent disruption-induced changes in available 3PL capacity, and a two-stage stochastic winner determination (WD) model is formulated to minimize the expected total procurement cost while jointly accounting for timeliness requirements, resilience strategy configuration, and carbon emission control. To address the computational burden associated with large-scale disruption scenarios, a hybrid algorithm-integrating scenario reduction (SR) with scenario-sorting-based dual decomposition and Lagrangian relaxation (SSDDLR), termed SR-SSDDLR, is developed. SR is employed to construct a feasible upper bound, and SSDDLR is used to obtain an effective lower bound. Finally, numerical experiments and a case study using real-world data from liner shipping routes are conducted to assess the proposed model, hybrid resilience strategy, and SR-SSDDLR algorithm and to derive managerial insights that support 4PLs in coordinating multiple 3PL resources and developing LSSP plans that balance greenness, timeliness, and resilience. The main contributions are summarized as follows:

1. Although WD models are used in TSP, the joint effects of disruption-induced capacity losses, deviation costs under soft time windows, and carbon emission caps remain insufficiently examined in LSSP. These elements are incorporated into a unified WDP framework to characterize their effects on greenness, timeliness, and resilience under disruptions.

2. A hybrid resilience strategy comprising multilevel fortification, capacity reservation, and emergency outsourcing is integrated with multi-3PL sourcing in the proposed WDP. Winner determination and transportation task allocation are jointly optimized to coordinate predisruption preparedness with postdisruption response.

3. A two-stage stochastic WD model is formulated to coordinate first-stage service procurement and resilience decisions with postdisruption transportation adjustments and is subsequently reformulated as a mixed-integer linear programming model. An SR-SSDDLR hybrid algorithm integrating SR and SSDDLR is developed to improve computational efficiency and solution quality when large numbers of disruption scenarios are considered.

4. A case study using data from real-world liner shipping routes is conducted to evaluate the effectiveness and applicability of the proposed model, hybrid resilience strategy, and SR-SSDDLR algorithm. Managerial insights are derived to support 4PLs in coordinating multiple 3PL resources for sustainable and resilient LSSP under disruption risk.

The remainder of this paper is organized as follows. Sections 2–4 review the relevant literature, present the research problem and mathematical model, and describe the solution method, respectively. Section 5 reports the numerical experiments and real-world case study, and Section 6 concludes the paper and outlines future research.

2. Literature review

In logistics service procurement auctions, WDP is a central decision problem for 4PLs, involving service provider selection and transportation task allocation within a combinatorial reverse auction (CRA) framework. Combinatorial bidding allows carriers to express preferences for combinations of transportation tasks and exploit economies of scope, and service requirements beyond price can also be incorporated into procurement decisions [10]. Hasan et al. [11] reviewed combinatorial auctions in transportation procurement, examining mathematical formulations and solution approaches and identifying sustainability, risk mitigation, and parameter uncertainty as directions for further research. Early WD models were largely formulated under deterministic settings, with emphasis placed on transportation task allocation, procurement cost control, and provider selection efficiency. As uncertainty increases in logistics demand, shipment volumes, carrier capacity, and disruptions, deterministic WD models become less capable of supporting robust decisions in complex transportation service procurement. Accordingly, the relevant literature is categorized into studies on WDP under parameter uncertainty and disruption risk, with further attention paid to sustainability, resilience strategies, and timeliness constraints.

2.1. Winner determination in service procurement auctions under uncertainty

2.1.1. WDP under parameter uncertainty

Parameter uncertainty is an important factor affecting the robustness of WDP decisions in logistics service procurement. In transportation service procurement, parameters such as logistics demand, shipment volumes, carrier capacities, bids, and procurement budgets are often subject to fluctuations. If these uncertainties are ignored, deterministic WD models may lead to capacity shortages, procurement cost overruns, or infeasible task allocations during implementation. Accordingly, WDP under parameter uncertainty is primarily addressed through stochastic programming, robust optimization, and uncertain programming to enhance the robustness and adaptability of logistics service procurement decisions. Specifically, existing studies can be broadly categorized into two streams: uncertainty in transportation tasks and supply capacity, and extensions involving budget constraints and bidding mechanisms.

Regarding uncertainty in transportation demand and supply capacity, existing studies mainly examine how fluctuations in shipment volumes, logistics demand, and carrier capacities affect task allocation and service provider selection. Ma et al. [12] formulated a two-stage stochastic integer programming WD model for truckload procurement under shipment uncertainty, offering an early stochastic programming framework for uncertain shipment volumes in transportation service procurement. Remli and Rekik [13] introduced a robust optimization model for combinatorial transportation auctions under uncertain shipment volumes, providing a robust method for shipment allocation. Subsequently, Zhang et al. [14] formulated a two-stage robust WD model for truckload service procurement under shipment volume uncertainty to enhance the robustness of procurement decisions. Remli et al. [15] further incorporated uncertainties in both shipment volumes and carrier capacities into the WDP and developed an improved constraint generation algorithm, which enhanced computational efficiency and model applicability in complex uncertain environments. Recently, Qian et al. [3] considered demand uncertainty in transportation service procurement auctions and

formulated a two-stage stochastic WD model combining sustainability and flexibility. A solution method combining dual decomposition and Lagrangian relaxation (DDLR) with sample-average approximation (SAA) was developed. Overall, WDP research under parameter uncertainty has gradually extended from cost-oriented optimization to broader operational and sustainability considerations.

With respect to budget constraints and bidding mechanisms, existing studies mainly examine the effects of procurement budgets, uncertain bid prices, and quantity discounts on procurement cost control and winner determination. Safari and Dolati [16] examined WDP under uncertain bid prices in general combinatorial auctions. Using uncertainty theory, the uncertain WDP was transformed into a deterministic maximum-weight clique formulation, providing an alternative approach to WD modeling under bid price uncertainty. Building on shipment volume uncertainty, Li et al. [17] further incorporated a purchase budget constraint into the WDP for transportation procurement and showed that the constraint can directly affect both the service bundles available to buyers and buyers' exposure to procurement cost overruns. Qian et al. [18] developed a two-stage stochastic nonlinear WD model for logistics service procurement auctions involving demand uncertainty and quantity discounts. The effects of quantity discounts on procurement costs and winner determination decisions were analyzed, revealing the relationships among procurement volume, quantity-discount bids, and task allocation outcomes. Together, these studies extend WDP research on cost control and bidding mechanisms by considering uncertain bid prices, purchase budgets, and quantity discounts. Beyond procurement auctions, Fu et al. [19] formulated a stochastic programming model for distributed flexible job shop scheduling with random processing times and developed a simulation-evaluated evolutionary algorithm to minimize makespan and total tardiness.

Overall, WDP studies under parameter uncertainty improve the robustness of procurement decisions by considering uncertainty in demand, shipment volumes, and carrier capacities together with budget constraints and bidding mechanisms. However, existing studies mainly focus on routine operational parameter fluctuations and the resulting effects on procurement costs and task allocation, whereas limited attention is paid to disruption-induced losses of 3PL service capacity or service unavailability. As disruptions can directly impair the fulfillment capability of winning service providers and further alter task allocation and risk-response decisions, WD modeling under disruption risk and the design of resilience strategies need to be further investigated.

2.1.2. WDP under disruption risk

In addition to parameter uncertainty, the robustness of WD decisions in logistics service procurement is affected by disruption risk. Available 3PL transportation capacity may be reduced, or transportation services may even be disrupted, by natural disasters, equipment failures, port congestion, malicious attacks, labor disputes, and carrier failures, affecting winner determination, task allocation, procurement costs, and service reliability. In LSSP, additional decision-making challenges in task reallocation, emergency outsourcing, and timeliness are posed by disruption-induced reductions in available 3PL capacity. Accordingly, the effects of disruptions on available 3PL capacity and service reliability need to be characterized in WDP research, with further attention paid to resilience strategy configuration, solution methods for large-scale disruption scenarios, and flexible timeliness mechanisms such as soft time windows.

Research on supply chain risk management provides a theoretical foundation for identifying, assessing, and modeling disruption risks in logistics systems. Kleindorfer and Saad [20] were among the first researchers to address disruption risk identification, assessment, and mitigation from a supply-chain risk-management perspective and provided a basic framework for subsequent disruption-risk modeling. Building on supply-chain risk-management research, disruption risk was gradually incorporated into WD models for logistics-service procurement. Qian et al. [21] considered 3PL-disruption risk in a two-stage stochastic WD model from a 4PL perspective, in which disruption-induced service capacity losses were incorporated into winner determination and task allocation decisions. Yin et al. [22] further considered the combined effects of disruption risk and quantity discounts and developed a stochastic nonlinear WD model, which was subsequently converted into a mixed-integer linear programming (MILP) model through linearization. As the disruption-scenario count increases, the numbers of variables and constraints in WD models can increase rapidly, making scenario reduction, sample average approximation, and decomposition algorithms important approaches for solving large-scale WD models more efficiently. Zhang et al. [23] and Bertsimas and Mundru [24] developed optimization-based scenario-reduction approaches for large-scale stochastic programs, offering methodological support for scenario compression and efficient solutions of WD models under large-scale disruption scenarios. Recently, Yin et al. [25] developed a sampling-based WD model for logistics service procurement from a 4PL perspective under joint disruption and demand uncertainty, incorporating temporary outsourcing and fortification into the risk mitigation framework. Overall, existing disruption-aware WDP studies primarily examine 3PL capacity losses, task reallocation, procurement costs, and resilience responses.

2.2. Disruption mitigation strategies

Research on disruption-mitigation strategies increasingly emphasizes the integrated deployment of multiple strategies rather than individual risk-mitigation measures. Jabbarzadeh et al. [26] considered facility and supply–demand disruptions in resilient supply chain network design and incorporated fortification investments into a hybrid robust-stochastic optimization framework, showing that protective investment can mitigate disruption effects. Subsequently, Sawik [27] investigated supply-chain disruption mitigation and recovery from a portfolio optimization perspective and showed that the coordinated deployment of multiple risk-response measures can enhance supply-chain resilience and reduce disruption losses. In WDP research on TSP, Qian et al. [28] examined provider-level sustainability and responsiveness in winner determination under accidental disruptions and combined fortification with temporary outsourcing to mitigate disruption effects. In addition to WDP-specific studies, research on resilient 4PL network design provides a complementary perspective on the design of hybrid mitigation strategies under disruption risk. Zhou et al. [29] proposed a hybrid mitigation strategy for resilient 4PL network design under disruption risk by integrating multilevel fortification, backup capacity, temporary outsourcing, multisourcing, and multiple transportation routes, providing a basis for the hybrid resilience strategy considered in this study. In electric-vehicle battery-recycling network design, Yin et al. [30] used combinatorial reverse auctions to select third-party recyclers under uncertainty in the quantities of retired batteries. Wang et al. [31] examined the implications of integrating winner determination into recycling-network design for network resilience. In a related 4PL-driven recycling setting, multilevel facility fortification and capacity reservation were incorporated to address disruption risks alongside carbon-emission and

service-time requirements [32]. These network-level studies provide a complementary perspective on resilience strategy design. However, the interactions among emergency outsourcing, capacity reservation, and multilevel fortification in liner-shipping service procurement WDPs remain insufficiently characterized.

2.3. Greenness and timeliness in TSP

Under disruption risk, reductions in available 3PL capacity may require 4PLs to reallocate transportation tasks or use emergency outsourcing, affecting both timeliness and transportation carbon emissions. Research on timeliness and carbon-emission control in TSP therefore provides an important basis for incorporating soft time-window penalties and a carbon emission cap into the WDP framework of this study. Hu et al. [33] incorporated transit time into TSP and formulated a bi-objective integer programming model to simultaneously minimize procurement cost and transit time, highlighting transit time as an important criterion in procurement decisions. Lee et al. [34] investigated global liner-service procurement using liner-service schedules to optimize carrier selection and procurement decisions, highlighting the importance of service schedules and timeliness for procurement robustness and operating costs. Yang et al. [35] incorporated lane-service time windows into TSP and developed an MILP model with a two-stage solution method, further highlighting the role of time-window constraints in resource allocation and outsourcing decisions.

In addition to timeliness requirements, the environmental performance of transportation services is an important consideration in procurement decisions. Jothi Basu et al. [36] examined carrier assignments in full-truckload procurement and showed how combinatorial bidding could reduce empty haul and carbon emissions. Triki et al. [37] further incorporated carbon-tax and cap-and-offset regulations into WDP models and allowed discounted bids for early shipments to improve load consolidation and reduce empty movements and carbon emissions. Zhou et al. [4] subsequently developed a two-stage stochastic WDP model under demand uncertainty that incorporates a carbon-emission cap and time-window constraints to address sustainability and timeliness. The studies of Jothi Basu et al., Triki et al., and Zhou et al. indicate that environmental performance depends not only on which carriers are selected but also on how transportation tasks are allocated.

Overall, existing studies establish the importance of greenness and timeliness in TSP. However, explicit carbon-emission control and soft time-window deviation costs remain insufficiently integrated with disruption-induced 3PL capacity losses and hybrid resilience strategy configuration. This gap motivates a unified WDP framework that coordinates greenness, timeliness, and resilience under disruptions.

Table 1 compares the present study with representative WDP studies relevant to logistics-service procurement in terms of uncertainty types, timeliness constraints, carbon-emission control, mitigation strategies, key modeling features, and solution methods.

Table 1. Comparison of representative WDP studies relevant to logistics-service procurement.

Article	Uncertainty type		Timeliness constraints		Carbon emission control	Mitigation strategies			Key modeling features	Solution methods
	Parameter	Disruption	Rigid constraints	Soft time windows		Outsourcing	Reservation	Multilevel fortification		
Ma et al. [12]	✓	—	—	—	—	—	—	—	Shipment uncertainty	Two-stage SP, MILP
Remli and Rekik [13]	✓	—	—	—	—	—	—	—	Robust allocation under shipment uncertainty	RO, CG
Zhang et al. [14]	✓	—	—	—	—	—	—	—	Truckload shipment volume uncertainty	Two-stage RO
Remli et al. [15]	✓	—	—	—	—	—	—	—	Shipment–carrier capacity uncertainty	RO, improved CG
Qian et al. [21]	—	✓	—	—	—	✓	✓	—	3PL capacity loss from a 4PL perspective	Two-stage SP, SR, CPLEX
Yin et al. [22]	—	✓	—	—	—	✓	—	—	Quantity discounts	Stochastic nonlinear WDP, MILP
Qian et al. [28]	—	✓	—	—	—	✓	—	—	Sustainability and responsiveness	Two-stage SP, scenario approximation
Lau and Li [38]	—	—	✓	—	—	—	—	—	Pickup-and-delivery time windows	WDP with time windows: modeling and solution
Safari and Dolati [16]	✓	—	—	—	—	—	—	—	Uncertain bid prices	Uncertain programming, MWCP
Qian et al. [3]	✓	—	—	—	—	✓	—	—	Sustainability and flexibility	Two-stage SP, SAA, DDLR
Li et al. [17]	✓	—	—	—	—	✓	—	—	Procurement budget	Sample-based RO, MILP
Qian et al. [18]	✓	—	—	—	—	✓	—	—	Quantity discounts	Two-stage SP, SAA, linearization
Triki et al. [37]	—	—	✓	—	✓	—	—	—	Carbon regulations and discounted bids	MILP
Yin et al. [25]	✓	✓	—	—	—	✓	—	—	Demand–disruption uncertainty	Sampling-based WDP, improved SAA
Zhou et al. [4]	✓	—	✓	—	✓	✓	—	—	Sustainability and timeliness	Two-stage SP, SAA, decomposition algorithm
Wang et al. [31]	—	✓	—	—	—	✓	✓	—	Resilient winner determination in a closed-loop supply chain	Two-stage SP, MILP, scenario-reduction-based decomposition algorithm
This study	—	✓	—	✓	✓	✓	✓	✓	Soft time-windows/carbon control/hybrid resilience strategy	Two-stage SP, SR-SSDDLR

Note: "✓" denotes a dimension that is explicitly modeled or treated as a primary focus, whereas "—" denotes a dimension receiving limited attention. RO, SP, CG, SAA, SR, LR, DDLR, SSDDLR, MILP, and MWCP denote robust optimization, stochastic programming, constraint generation, sample average approximation, scenario reduction, Lagrangian relaxation, dual decomposition and Lagrangian relaxation, scenario-sorting-based dual decomposition and Lagrangian relaxation, mixed-integer linear programming, and the maximum-weight clique problem, respectively.

2.4. Research gaps

As shown in Table 1, studies relevant to the WDP in logistics-service procurement have examined uncertainty modeling, disruption risk, sustainability, timeliness, resilience strategies, and solution methods. However, these dimensions remain only partially integrated in LSSP under disruption risk, leaving four main research gaps.

First, existing disruption-aware WDP studies incorporate service capacity losses and resilience responses, but explicit carbon emission control remains insufficiently examined. Consequently, the relationships among disruption-induced reductions in available 3PL capacity, carbon emissions, winner determination, transportation-task allocation, and timeliness remain insufficiently characterized in LSSP.

Second, existing TSP studies usually represent timeliness through deterministic service-time requirements or rigid time-window constraints. Soft time windows permit early or late task completion and quantify the associated costs but have received limited attention under disruption risk.

Third, existing WDP studies generally employ individual resilience measures or partial strategy combinations. The coordinated configuration of multilevel fortification, capacity reservation, and emergency outsourcing across predisruption protection and postdisruption response remains insufficiently studied.

Fourth, large-scale disruption scenarios lead to substantial increases in the numbers of variables and constraints in two-stage stochastic WD models. This growth creates a need for efficient solution methods tailored to the combinatorial winner-determination structure, two-stage decision process, and hybrid resilience-strategy configuration.

To address these research gaps, a WDP for LSSP under disruption risk is investigated from a 4PL perspective by integrating greenness, timeliness, and resilience within a unified decision framework. A two-stage stochastic WD model is formulated to integrate disruption-induced reductions in available 3PL capacity, carbon-emission control, winner determination, and transportation-task allocation within a unified decision framework, with soft time windows incorporated to quantify earliness and tardiness costs. A hybrid resilience strategy comprising emergency outsourcing, capacity reservation, and multilevel fortification is developed to coordinate predisruption protection and postdisruption response. An SR-SSDDLR algorithm is developed to address the computational burden created by large-scale disruption scenarios.

3. Problem description and model formulation

LSSP organized by a 4PL through a CRA platform is considered. The 4PL aggregates transportation tasks submitted by shippers and announces the transportation demands, service-time requirements, and auction rules. Candidate 3PLs then submit bundle bids reflecting route coverage, available transportation capacity, expected task-completion times, carbon-emission factors, and cost structures. Each bundle bid may cover one or more transportation tasks. The winning 3PLs and the corresponding bundle bids are jointly selected by the 4PL, and the transportation tasks are allocated accordingly. Thus, 3PL selection, bundle-bid selection, and transportation task-allocation constitute interdependent decisions within the WDP. Figure 1 illustrates the procurement process, including the announcement of transportation demands, submission of bundle bids, winner determination, and transportation task allocation.

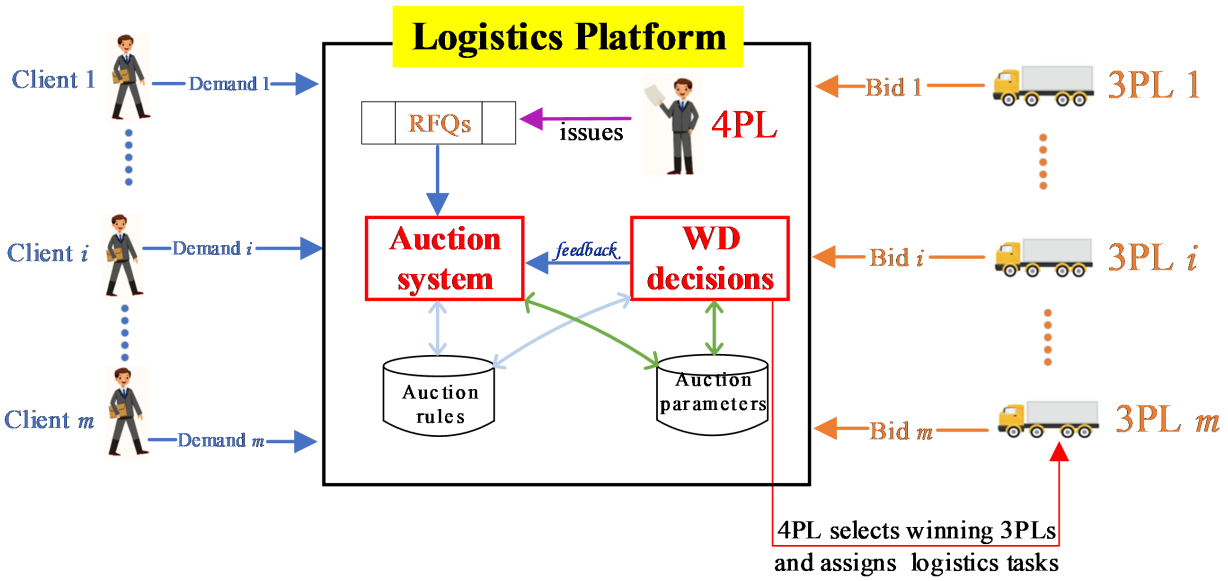


Figure 1. CRA process for LSSP on a 4PL platform.

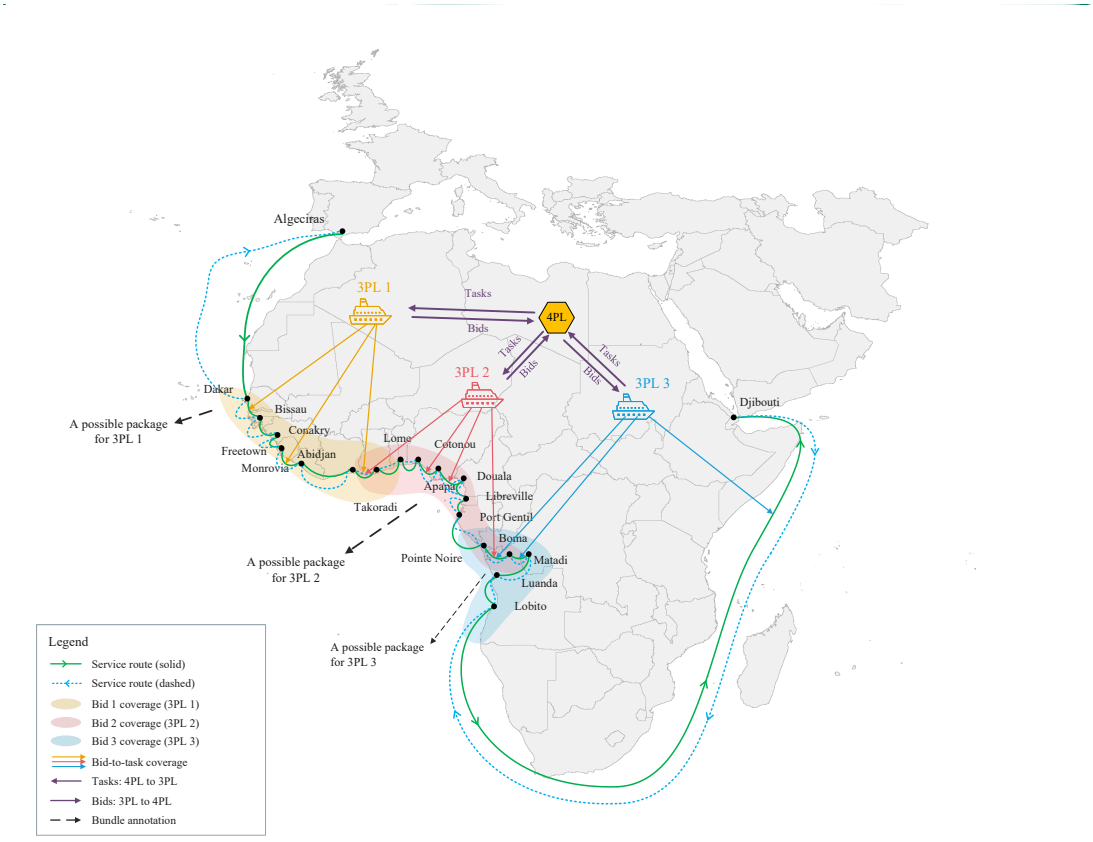


Figure 2. Bundle-bid coverage of transportation tasks in the 4PL–CRA framework.

As shown in Figure 2, candidate 3PLs may construct bundle bids based on serviceable ports and routes and available transportation resources. Each bundle bid specifies the covered transportation tasks and routes, capacity range, unit bid price, expected task-completion time, and carbon-emission

factor. A bundle bid can cover multiple transportation tasks, and the same task can be covered by bids submitted by different 3PLs. Within the prescribed lower and upper limits on the number of winning bids, the 4PL selects 3PLs and their bundle bids to integrate route coverage and transportation capacity across different service providers. Because bundle bids submitted by the same 3PL are mutually exclusive, at most one bundle bid from each 3PL can be selected. In this study, the demand d_i of transportation task i is divisible and can be fulfilled by multiple winning 3PLs. The transportation volume assigned to each winning bundle bid contributes to satisfying the demand of each task it covers. When multiple winning bids cover the same task, their transportation volumes, together with any emergency outsourcing, satisfy its demand. Transportation volumes are determined after the disruption scenario is realized.

Figure 3 illustrates the coverage relationships and transportation volume allocation for three tasks connecting Ports A, B, C, and D, with respective demands of 40, 100, and 60 units. Bid 1 submitted by 3PL 1 covers all three tasks, whereas Bids 2 and 3 submitted by 3PLs 2 and 3 cover Tasks 1–2 and Tasks 2–3, respectively, with dashed lines indicating the task–bid coverage relationships. In the illustrated procurement plan, Bids 2 and 3 are selected, whereas Bid 1 is not selected. Under a given scenario, assigning transportation volumes of 40 and 60 units to Bids 2 and 3, respectively, satisfies the demands of Tasks 1 and 3, whereas the two 3PLs contribute 40 and 60 units to jointly fulfill the 100-unit demand of Task 2.

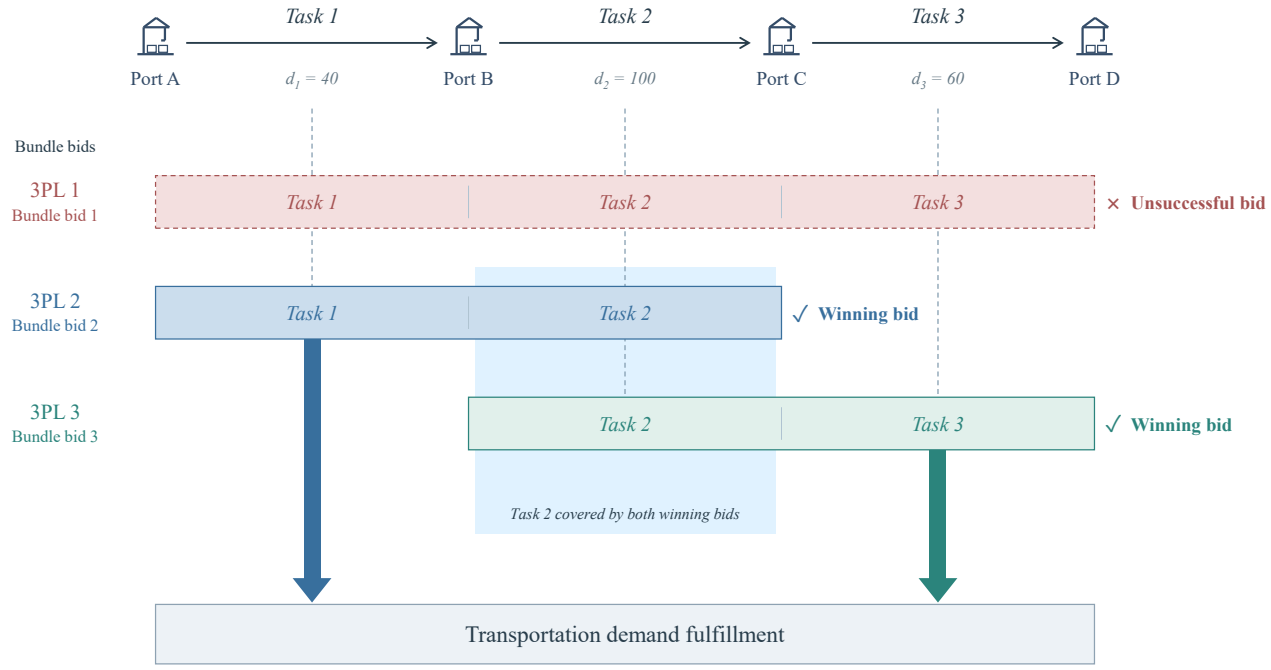


Figure 3. An example of overlapping bundle bids and transportation demand fulfillment.

During procurement-plan implementation, unexpected disruptions such as waterway blockages, port congestion, natural disasters, and carrier-service failures may reduce the transportation capacity available from some winning bundle bids. Consequently, transportation demand may exceed the capacity available under the predisruption procurement plan. In addition, task completion times vary across bundle bids, and task completion before or after shipper-preferred time windows incurs corresponding time-deviation costs. Therefore, changes in available 3PL capacity and the resulting

adjustments in transportation allocation may affect carbon emissions, procurement cost, timeliness, and disruption response, all of which should be considered jointly in the LSSP under disruption risk. To mitigate disruption-induced capacity losses, a hybrid resilience strategy comprising multilevel fortification, capacity reservation, and emergency outsourcing is considered. Multilevel fortification assigns different protection levels to increase the proportion of transportation capacity retained by winning bundle bids under disruption scenarios. Capacity reservation is a predisruption decision made for winning bundle bids. Within the reservable-capacity limit of each bid, the 4PL reserves additional capacity in advance to supplement the basic capacity retained after a disruption. Emergency outsourcing is a recourse decision determined after the disruption scenario is realized to meet residual task demand beyond the available capacity of the winning 3PLs.

Under this decision setting, a WDP for LSSP under stochastic disruption risk and soft time windows is formulated. The winning 3PLs and bundle bids, fortification levels, and capacity reservation amounts are jointly determined before disruptions, whereas transportation allocations and emergency outsourcing decisions are adjusted after each disruption scenario is realized. The expected total procurement cost is minimized subject to transportation demand, service capacity, timeliness, and carbon emission requirements. Table 2 summarizes the relevant sets, parameters, and decision variables.

Table 2. Notation and definitions.

Notation	Definition
Sets	
I	Set of transportation tasks between origin and destination ports on the shipping routes, indexed by i.
J	Set of candidate 3PL providers participating in the procurement auction, indexed by j.
Ω	Set of disruption scenarios representing the disruption states of bundle bids, indexed by w.
L	Set of available fortification levels for bundle bids, indexed by l.
K_j	Set of bundle bids submitted by 3PL j, indexed by k.
Parameters	
$C_{\max}$	Maximum budget for fortification and capacity reservation.
B	A sufficiently large positive constant.
$N_{\min}$	Minimum number of winning 3PL providers.
$N_{\max}$	Maximum number of winning 3PL providers, where $N_{\max} > N_{\min}$.
LS_{jk}	Minimum transportation volume specified in bundle bid k submitted by 3PL j, $j \in J,\ k \in K_j$.
US_{jk}	Maximum transportation volume specified in bundle bid k submitted by 3PL j, $j \in J,\ k \in K_j$.
e_i	Unit emergency outsourcing cost for transportation task i, $i \in I$.
b_{jk}	Unit bid price of bundle bid k submitted by 3PL j, $j \in J,\ k \in K_j$.
CE_{jk}	Carbon emission factor per unit of transportation volume under bundle bid k submitted by 3PL j, $j \in J,\ k \in K_j$.
CE_i^O	Carbon emission factor per unit of emergency outsourcing volume for transportation task i, $i \in I$.
Cap	Maximum total carbon emissions permitted in each disruption scenario.
c_{jkl}	Fixed cost of fortifying bundle bid k of 3PL j at level l, $j \in J,\ k \in K_j,\ l \in L$.
d_i	Transportation demand associated with task i, $i \in I$.
u_{jk}	Unit capacity reservation cost for bundle bid k of 3PL j, $j \in J,\ k \in K_j$.
q_{jkw}	Binary parameter equal to 1 if bundle bid k of 3PL j is disrupted in scenario w, and 0 otherwise, $j \in J,\ k \in K_j,\ w \in \Omega$.
a_{ijk}	Binary parameter equal to 1 if transportation task i can be served by bundle bid k of 3PL j, and 0 otherwise, $i \in I,\ j \in J,\ k \in K_j$.
r_w	Occurrence probability of disruption scenario w, $w \in \Omega$.
v_j	Relationship management cost associated with selecting 3PL j, $j \in J$.
$T_{\min,i}$	Earliest preferred arrival time for transportation task i, $i \in I$.
$T_{\max,i}$	Latest preferred arrival time for transportation task i, $i \in I$.
t_{ijk}	Completion time of transportation task i when served by bundle bid k of 3PL j, $i \in I,\ j \in J,\ k \in K_j$.

Table 2. Notation and definitions (continued).

Notation	Definition
α_i	Earliness penalty coefficient for transportation task i, $i \in I$.
β_i	Tardiness penalty coefficient for transportation task i, $i \in I$.
A_{jk}	Maximum reservable capacity of bundle bid k submitted by 3PL j, $j \in J,\ k \in K_j$.
ψ_{jkl}	Proportion of transportation capacity retained under disruption when bundle bid k of 3PL j is fortified at level l, $j \in J,\ k \in K_j,\ l \in L$.
Decision variables	
Z_{ijk}	Non-negative auxiliary variable representing the earliness deviation of transportation task i associated with selecting bundle bid k of 3PL j, $i \in I,\ j \in J,\ k \in K_j$.
Q_{ijk}	Non-negative auxiliary variable representing the tardiness deviation of transportation task i associated with selecting bundle bid k of 3PL j, $i \in I,\ j \in J,\ k \in K_j$.
h_{jkl}	Binary variable equal to 1 if bundle bid k of 3PL j is fortified at level l, and 0 otherwise, $j \in J,\ k \in K_j,\ l \in L$.
δ_{jk}	Capacity reserved for bundle bid k of 3PL j, $j \in J,\ k \in K_j$.
y_{jkw}	Actual transportation volume assigned to bundle bid k of 3PL j under disruption scenario w, $j \in J,\ k \in K_j,\ w \in \Omega$.
p_{jk}	Binary variable equal to 1 if bundle bid k submitted by 3PL j is selected as a winning bid, and 0 otherwise, $j \in J,\ k \in K_j$.
ϕ_{iw}	Emergency outsourcing volume allocated to transportation task i under disruption scenario w, $i \in I,\ w \in \Omega$.

Using the notation in Table 2, we formulate a two-stage stochastic WD model that minimizes the expected total procurement cost. Specifically, under the two-stage stochastic programming framework, first-stage decisions are made before a disruption scenario w is realized, including 3PL bundle-bid selection, fortification-level selection, and capacity reservation, represented by p_{jk}, h_{jkl}, and δ_{jk}, respectively. Second-stage decisions are made after the disruption scenario is realized, including the actual transportation quantity y_{jkw} and the emergency outsourcing quantity ϕ_{iw}. Under the two-stage structure, service provider selection, protective investment, and capacity reservation are determined before disruptions, whereas transportation allocation and emergency outsourcing are adjusted after the disruption-specific available capacity becomes known. The model simultaneously incorporates soft time-window penalties, a carbon-emission cap, 3PL transportation-capacity limits, emergency outsourcing, capacity reservation, and multilevel fortification.

Model (P1)

$$\min_{\mathbf{h},\mathbf{p},\boldsymbol{\delta},\mathbf{Z},\mathbf{Q}} \quad \sum_{l\in L}\sum_{j\in J}\sum_{k\in K_j} c_{jkl}h_{jkl} + \sum_{j\in J}\sum_{k\in K_j} v_j p_{jk} + \sum_{j\in J}\sum_{k\in K_j} u_{jk}\delta_{jk} + \sum_{j\in J}\sum_{k\in K_j}\sum_{i\in I}(\alpha_i Z_{ijk} + \beta_i Q_{ijk}) + \mathrm{E}_w f(\mathbf{h},\mathbf{p},\boldsymbol{\delta},\mathbf{Z},\mathbf{Q},\mathbf{w}) \tag{3.1}$$

$$\text{s.t.} \quad \sum_{l\in L}\sum_{j\in J}\sum_{k\in K_j} c_{jkl}h_{jkl} + \sum_{j\in J}\sum_{k\in K_j} u_{jk}\delta_{jk} \le C_{\max}, \tag{3.2}$$

$$Z_{ijk} \ge T_{\min,i} - \{(1-a_{ijk})T_{\min,i} + a_{ijk}[(1-p_{jk})T_{\min,i} + p_{jk}t_{ijk}]\}, \quad \forall i \in I, j \in J, k \in K_j, \tag{3.3}$$

$$Q_{ijk} \ge \{(1-a_{ijk})T_{\max,i} + a_{ijk}[(1-p_{jk})T_{\max,i} + p_{jk}t_{ijk}]\} - T_{\max,i}, \quad \forall i \in I, j \in J, k \in K_j, \tag{3.4}$$

$$\sum_{k\in K_j} p_{jk} \le 1, \quad \forall j \in J, \tag{3.5}$$

$$\sum_{j\in J}\sum_{k\in K_j} p_{jk} \le N_{\max}, \tag{3.6}$$

$$\sum_{j\in J}\sum_{k\in K_j} p_{jk} \ge N_{\min}, \tag{3.7}$$

$$\delta_{jk} \le B p_{jk}, \quad \forall j \in J, k \in K_j, \tag{3.8}$$

$$\sum_{l\in L} h_{jkl} \le p_{jk}, \quad \forall j \in J, k \in K_j, \tag{3.9}$$

$$\delta_{jk} \le A_{jk}, \quad \forall j \in J, k \in K_j, \tag{3.10}$$

$$Z_{ijk} \ge 0, \quad \forall i \in I, j \in J, k \in K_j, \tag{3.11}$$

$$Q_{ijk} \ge 0, \quad \forall i \in I, j \in J, k \in K_j, \tag{3.12}$$

$$\delta_{jk} \ge 0, \quad \forall j \in J, k \in K_j, \tag{3.13}$$

$$h_{jkl} \in \{0,1\}, \quad \forall j \in J, k \in K_j, l \in L, \tag{3.14}$$

$$p_{jk} \in \{0,1\}, \quad \forall j \in J, k \in K_j, \tag{3.15}$$

where

$$f(\mathbf{h}, \mathbf{p}, \boldsymbol{\delta}, \mathbf{Z}, \mathbf{Q}, \mathbf{w}) = \sum_{j\in J}\sum_{k\in K_j} b_{jk} y_{jkw} + \sum_{i\in I} e_i \phi_{iw}. \tag{3.16}$$

$$\sum_{j\in J}\sum_{k\in K_j} a_{ijk} y_{jkw} + \phi_{iw} = d_i, \quad \forall i \in I, w \in \Omega, \tag{3.17}$$

$$q_{jkw}\left(\sum_{l\in L} h_{jkl}\psi_{jkl}\right) US_{jk} + (1 - q_{jkw}) US_{jk} \ge y_{jkw} - \delta_{jk}, \quad \forall j \in J, k \in K_j, w \in \Omega, \tag{3.18}$$

$$q_{jkw} \min\left\{\left(\sum_{l\in L} h_{jkl}\psi_{jkl}\right) US_{jk}, LS_{jk}\right\} + (1 - q_{jkw}) p_{jk} LS_{jk} \le y_{jkw}, \quad \forall j \in J, k \in K_j, w \in \Omega, \tag{3.19}$$

$$B p_{jk} \ge y_{jkw}, \quad \forall j \in J, k \in K_j, w \in \Omega, \tag{3.20}$$

$$\sum_{j\in J}\sum_{k\in K_j} CE_{jk} y_{jkw} + \sum_{i\in I} CE_i^O \phi_{iw} \le \mathrm{Cap}, \quad \forall w \in \Omega, \tag{3.21}$$

$$y_{jkw} \ge 0, \quad \forall j \in J, k \in K_j, w \in \Omega, \tag{3.22}$$

$$\phi_{iw} \ge 0, \quad \forall i \in I, w \in \Omega. \tag{3.23}$$

In Model (P1), the objective function represents the expected total procurement cost of the 4PL, including first-stage fortification costs, 3PL management costs, capacity reservation costs, and soft time-window penalties as well as the expected transportation and emergency outsourcing costs incurred across different disruption scenarios in the second stage. Constraint (3.2) limits the total fortification and capacity reservation costs to the maximum budget for protective investment. Constraints (3.3) and (3.4) define the soft time windows and characterize earliness and tardiness deviations. Constraint (3.5) requires that at most one bundle bid can be selected for each 3PL.

Constraints (3.6) and (3.7) restrict the number of winning 3PLs to the range between $N_{\min}$ and $N_{\max}$. The upper bound controls the transportation-coordination and relationship-management burden associated with selecting too many 3PLs, and the lower bound ensures that the procurement plan includes multiple winning 3PLs rather than relying on a single provider. Sheffi [10] discussed the relationship between the number of carriers and management costs, providing a managerial rationale for imposing an upper bound. Remli and Rekik [13] explicitly imposed lower and upper bounds on the number of winning carriers in a combinatorial auction winner determination model, providing a modeling reference for the limits adopted in this study. Because Constraint (3.5) allows each 3PL to win at most one bundle bid, the total number of winning bids equals the number of winning 3PLs. Constraints (3.6) and (3.7) therefore limit the number of winning 3PLs through the total number of winning bids. Constraint (3.8) ensures that capacity reservation can only be assigned to selected 3PL bundle bids, where B is a sufficiently large constant. Constraint (3.9) ensures that fortification can only be applied to selected 3PL bundle bids and that at most one fortification level can be selected for each winning bundle bid. Constraint (3.10) specifies the upper bound on reserved capacity. Constraints (3.11)–(3.13) impose non-negativity requirements, and Constraints (3.14) and (3.15) define the binary decision variables. Equation (3.16) defines the second-stage objective function, which minimizes the transportation costs incurred by the winning 3PLs and the emergency outsourcing costs under each disruption scenario. Constraint (3.17) ensures that under each disruption scenario, the transportation volumes provided by winning bundle bids covering task i, together with the emergency outsourcing volume, sum to its demand d_i. Thus, the demand of a task can be fulfilled by multiple winning bids. Constraint (3.18) limits the transportation volume assigned to each winning bundle bid to the sum of the bid's scenario-dependent basic capacity and reserved capacity. The basic capacity is US_{jk} when the bid is not disrupted, and the capacity retained under disruption depends on the selected fortification level. In the model, reserved capacity δ_{jk} supplements the available basic capacity in both disrupted and undisrupted scenarios. Constraint (3.19) specifies the corresponding minimum transportation-volume requirement. Constraint (3.20) ensures that transportation tasks can only be allocated to winning 3PLs. Constraint (3.21) limits the total carbon emissions generated by transportation assignments to winning 3PLs and emergency outsourcing to the prescribed carbon-emission cap under each disruption scenario. Emissions from each source are calculated by multiplying the transportation volume by the corresponding emission factor. Total emissions are expressed in kg CO_2e, consistent with the unit of the emission cap. Finally, Constraints (3.22) and (3.23) impose non-negativity on transportation and outsourcing quantities.

Disruption risk is represented by discrete scenarios. For a given scenario w, $q_{jkw} = 0$ indicates that bundle bid k submitted by 3PL j operates normally, whereas $q_{jkw} = 1$ indicates that the bundle bid is disrupted. For illustration, three 3PLs, each submitting one bundle bid, are considered. The scenario vector $\mathbf{w} = [1, 0, 0]$ indicates that 3PL 1 is disrupted, whereas 3PLs 2 and 3 operate normally. Let Ω represent the set of disruption scenarios, Λ the set of all bundle bids exposed to disruption, Λ_w the subset of bundle bids disrupted under scenario w, and r_k the disruption probability of bundle bid $k \in \Lambda$. The disruption probability of each exposed bundle bid is treated as known, and the disruption states of different bundle bids are treated as mutually independent. Following Snyder and Daskin [39], the probability of scenario w is calculated as follows:

$$r_w = \prod_{k\in\Lambda_w} r_k \prod_{k\in\Lambda\setminus\Lambda_w} (1 - r_k). \tag{3.24}$$

Using the disruption-scenario probabilities calculated from Eq. (3.24), the two-stage stochastic WD model can be reformulated as the following MILP model, denoted by Model (P2).

Model (P2)

$$\begin{aligned}
\min_{\mathbf{h},\mathbf{p},\delta,\mathbf{Z},\mathbf{Q}} \quad & \sum_{l\in L}\sum_{j\in J}\sum_{k\in K_j} c_{jkl}h_{jkl} + \sum_{j\in J}\sum_{k\in K_j} v_j p_{jk} + \sum_{j\in J}\sum_{k\in K_j} u_{jk}\delta_{jk} \\
& + \sum_{j\in J}\sum_{k\in K_j}\sum_{i\in I}(\alpha_i Z_{ijk} + \beta_i Q_{ijk}) + \sum_{w\in\Omega} r_w \left(\sum_{j\in J}\sum_{k\in K_j} b_{jk}y_{jkw} + \sum_{i\in I} e_i\phi_{iw}\right) && (3.25)\\
\text{s.t.} \quad & \sum_{l\in L}\sum_{j\in J}\sum_{k\in K_j} c_{jkl}h_{jkl} + \sum_{j\in J}\sum_{k\in K_j} u_{jk}\delta_{jk} \le C_{\max}, && (3.26)\\
& Z_{ijk} \ge T_{\min,i} - \{(1 - a_{ijk})T_{\min,i} \\
& \quad + a_{ijk}[(1 - p_{jk})T_{\min,i} + p_{jk}t_{ijk}]\}, \quad \forall i \in I, j \in J, k \in K_j, && (3.27)\\
& Q_{ijk} \ge \{(1 - a_{ijk})T_{\max,i} \\
& \quad + a_{ijk}[(1 - p_{jk})T_{\max,i} + p_{jk}t_{ijk}]\} - T_{\max,i}, \quad \forall i \in I, j \in J, k \in K_j, && (3.28)\\
& \sum_{k\in K_j} p_{jk} \le 1, \quad \forall j \in J, && (3.29)\\
& \sum_{j\in J}\sum_{k\in K_j} p_{jk} \le N_{\max}, && (3.30)\\
& \sum_{j\in J}\sum_{k\in K_j} p_{jk} \ge N_{\min}, && (3.31)\\
& \delta_{jk} \le Bp_{jk}, \quad \forall j \in J, k \in K_j, && (3.32)\\
& \sum_{l\in L} h_{jkl} \le p_{jk}, \quad \forall j \in J, k \in K_j, && (3.33)\\
& \delta_{jk} \le A_{jk}, \quad \forall j \in J, k \in K_j, && (3.34)\\
& \sum_{j\in J}\sum_{k\in K_j} a_{ijk}y_{jkw} + \phi_{iw} = d_i, \quad \forall i \in I, w \in \Omega, && (3.35)\\
& q_{jkw}\left(\sum_{l\in L} h_{jkl}\psi_{jkl}\right) US_{jk} \\
& \quad + (1 - q_{jkw})US_{jk} \ge y_{jkw} - \delta_{jk}, \quad \forall j \in J, k \in K_j, w \in \Omega, && (3.36)\\
& q_{jkw}\min\left\{\left(\sum_{l\in L} h_{jkl}\psi_{jkl}\right) US_{jk}, LS_{jk}\right\} \\
& \quad + (1 - q_{jkw})p_{jk}LS_{jk} \le y_{jkw}, \quad \forall j \in J, k \in K_j, w \in \Omega, && (3.37)\\
& Bp_{jk} \ge y_{jkw}, \quad \forall j \in J, k \in K_j, w \in \Omega, && (3.38)\\
& \sum_{j\in J}\sum_{k\in K_j} CE_{jk}y_{jkw} + \sum_{i\in I} CE_i^O\phi_{iw} \le \text{Cap}, \quad \forall w \in \Omega, && (3.39)
\end{aligned}$$

$$y_{jkw} \geq 0, \quad \forall j \in J, k \in K_j, w \in \Omega, \tag{3.40}$$

$$\phi_{iw} \geq 0, \quad \forall i \in I, w \in \Omega, \tag{3.41}$$

$$Z_{ijk} \geq 0, \quad \forall i \in I, j \in J, k \in K_j, \tag{3.42}$$

$$Q_{ijk} \geq 0, \quad \forall i \in I, j \in J, k \in K_j, \tag{3.43}$$

$$\delta_{jk} \geq 0, \quad \forall j \in J, k \in K_j, \tag{3.44}$$

$$h_{jkl} \in \{0, 1\}, \quad \forall j \in J, k \in K_j, l \in L, \tag{3.45}$$

$$p_{jk} \in \{0, 1\}, \quad \forall j \in J, k \in K_j. \tag{3.46}$$

Constraint (3.39) limits the carbon emissions generated by transportation provided by winning 3PLs and emergency outsourcing in each disruption scenario.

Model (P2) is an MILP model that can be solved directly using commercial solvers, including CPLEX. However, as the disruption-scenario count increases, the numbers of constraints and decision variables increase rapidly, posing substantial computational challenges. Therefore, an SR-SSDDLR algorithm integrating SR and SSDDLR is developed in the next section to enhance computational efficiency for large-scale disruption scenarios.

4. Algorithm design

To address the computational difficulty of directly solving Model (P2) under large-scale disruption scenarios, an SR-SSDDLR hybrid algorithm is developed. Scenario reduction is used to obtain first-stage decisions, which are then evaluated over the full scenario set to obtain a feasible objective value and an upper bound. A lower bound is computed using SSDDLR to assess the quality of this solution. Figure 4 presents the overall algorithmic procedure, including scenario screening, multiplier updates, and the termination test. The algorithm proceeds as follows:

Algorithm 1. SR-SSDDLR procedure

1. Solve the scenario-reduction model (P3) to obtain the reduced scenario set and its probabilities, and solve Model (P4) to determine the first-stage decisions.
2. Fix the first-stage decisions, calculate the associated fixed cost, and solve the independent recourse subproblem for each scenario in the full scenario set. Add the fixed cost to the recourse costs weighted by the original scenario probabilities to obtain a feasible objective value, which provides an upper bound on the original problem.
3. Relax the nonanticipativity constraints, and solve the scenario subproblems at zero multipliers. Calculate and sort the scenario contributions in descending order, and screen scenarios according to their relative contributions. Preserve the zero-multiplier contributions of excluded scenarios for the final lower-bound calculation.
4. Initialize the Lagrangian multipliers, solve the retained-scenario subproblems, and record the current and best dual values. Compute the subgradient and step size, update the multipliers, and solve the updated subproblems before checking the termination criterion. Continue iterating if the criterion is not satisfied.
5. Add the zero-multiplier contributions of excluded scenarios to the best retained-scenario dual value to obtain the lower bound, and report the feasible objective value, the upper and lower bounds, and their relative optimality gap.

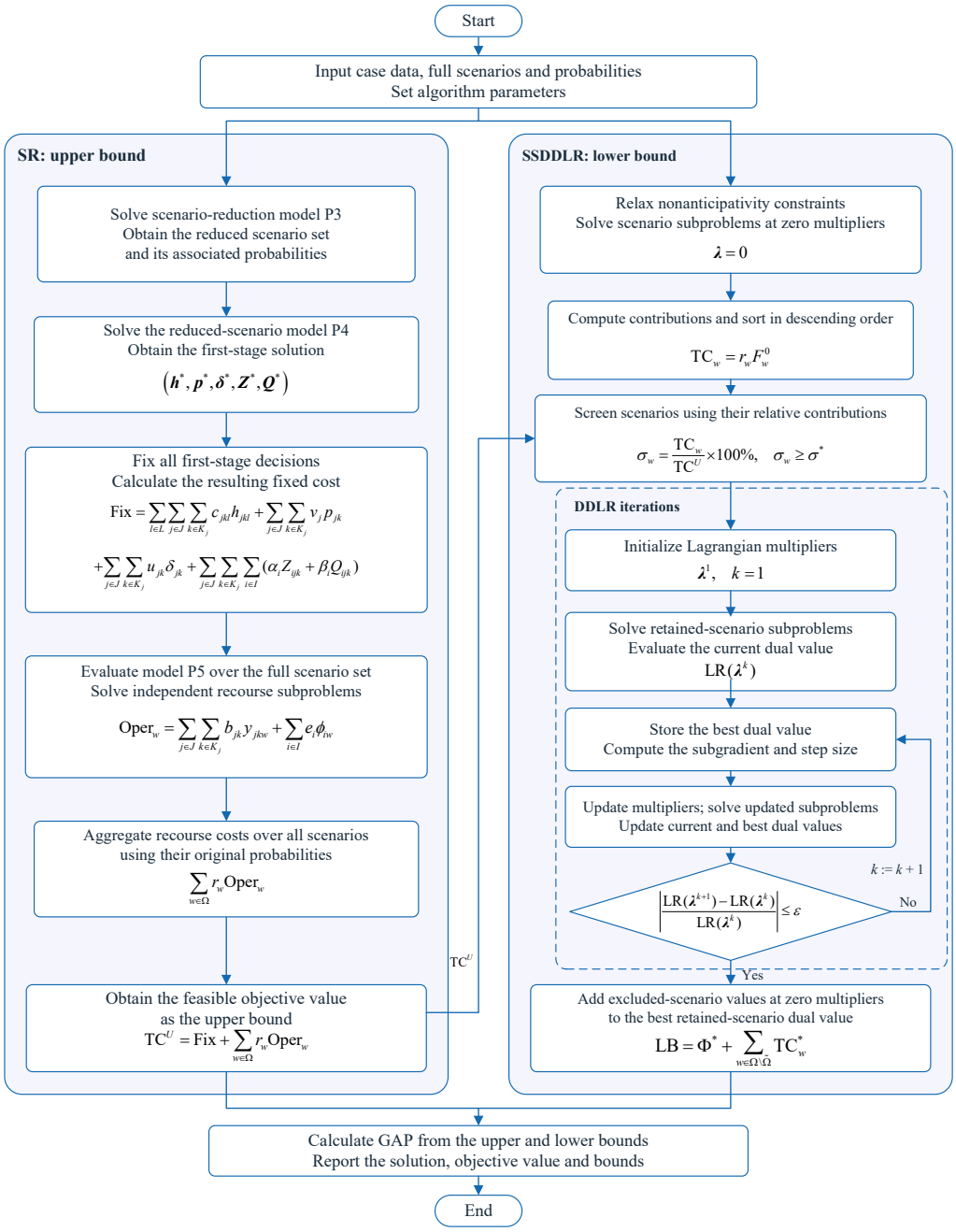


Figure 4. Flowchart of the SR-SSDDLR algorithm.

4.1. Upper-bound computation based on scenario reduction

Using the SR method, the full scenario set is approximated by a representative subset, thereby reducing computational complexity while retaining the main characteristics of the original scenario distribution. Let V denote the set of 3PL bundle bids potentially subject to disruption. The vector $\mathbf{v} = \{v_k\}_{1\cdots|V|}$ represents the uncertain disruption states of the bundle bids in V. Each v_k takes a binary realization $v_k^{\kappa_k} \in \{0,1\}$, where $v_k^{\kappa_k} = 0$ denotes normal operation, and $v_k^{\kappa_k} = 1$ denotes disruption. The probability assigned to realization $v_k^{\kappa_k}$ is denoted by $r_k^{\kappa_k}$, where $0 < \left|r_k^{\kappa_k}\right| < 1$; $\kappa_k = 1,2$; and $k = 1,2,\ldots,|V|$. The reduced disruption scenario set and the corresponding scenario probabilities can then be determined by the following model:

Model (P3)

$$\min \quad \sum_{\kappa_1=1}^{2}\sum_{\kappa_2=1}^{2}\cdots\sum_{\kappa_{|V|}=1}^{2}\left[\left(1 - r_1^{\kappa_1} r_2^{\kappa_2}\cdots r_{|V|}^{\kappa_{|V|}}\right)\widehat{\rho}_{\kappa_1,\kappa_2,\ldots,\kappa_{|V|}}\right] \tag{4.1}$$

$$\text{s.t.} \quad \sum_{\kappa_2=1}^{2}\sum_{\kappa_3=1}^{2}\cdots\sum_{\kappa_{|V|}=1}^{2}\widehat{\rho}_{\kappa_1,\kappa_2,\ldots,\kappa_{|V|}} = r_1^{\kappa_1}, \quad \kappa_1 = 1,2, \tag{4.2}$$

$$\sum_{\kappa_1=1}^{2}\sum_{\kappa_3=1}^{2}\cdots\sum_{\kappa_{|V|}=1}^{2}\widehat{\rho}_{\kappa_1,\kappa_2,\ldots,\kappa_{|V|}} = r_2^{\kappa_2}, \quad \kappa_2 = 1,2, \tag{4.3}$$

$$\vdots$$

$$\sum_{\kappa_1=1}^{2}\sum_{\kappa_2=1}^{2}\cdots\sum_{\kappa_{|V|-1}=1}^{2}\widehat{\rho}_{\kappa_1,\kappa_2,\ldots,\kappa_{|V|}} = r_{|V|}^{\kappa_{|V|}}, \quad \kappa_{|V|} = 1,2, \tag{4.4}$$

$$\sum_{\kappa_1=1}^{2}\sum_{\kappa_2=1}^{2}\cdots\sum_{\kappa_{|V|}=1}^{2}\widehat{\rho}_{\kappa_1,\kappa_2,\ldots,\kappa_{|V|}} = 1, \tag{4.5}$$

$$0 \le \widehat{\rho}_{\kappa_1,\kappa_2,\ldots,\kappa_{|V|}} \le 1, \quad \forall \kappa_1,\kappa_2,\ldots,\kappa_{|V|}, \tag{4.6}$$

where $\widehat{\rho}_{\kappa_1,\kappa_2,\ldots,\kappa_{|V|}}$ denotes the new probability associated with a disruption scenario. The objective function of Model (P3) includes both the probabilities of the original scenarios and those of the reduced scenarios, with the aim of retaining high-probability scenarios from the initial scenario set while reducing the number of scenarios. Constraints (4.2)–(4.4) require that for each potentially disrupted bundle bid, the probability of each disruption state is preserved across the original and reduced scenario sets. Constraint (4.5) requires that the probabilities of all scenarios in the reduced scenario set sum to one, and Constraint (4.6) restricts the probability of each reduced scenario to the interval $[0,1]$. By solving the linear programming problem in Model (P3) using CPLEX, the reduced-disruption scenario set $\widehat{\Omega}$ and the corresponding scenario probabilities $\widehat{\rho}_w$ are obtained. Model (P2) is then reformulated as Model (P4) using the reduced-disruption scenario set and the corresponding probabilities.

The reduced-scenario model used to obtain the first-stage solution $\left(\mathbf{h}^\star, \mathbf{p}^\star, \boldsymbol{\delta}^\star, \mathbf{Z}^\star, \mathbf{Q}^\star\right)$ is formulated as follows:

Model (P4)

$$\min_{\mathbf{h},\mathbf{p},\boldsymbol{\delta},\mathbf{Z},\mathbf{Q}} \quad \sum_{l\in L}\sum_{j\in J}\sum_{k\in K_j} c_{jkl}h_{jkl} + \sum_{j\in J}\sum_{k\in K_j} v_j p_{jk} + \sum_{j\in J}\sum_{k\in K_j} u_{jk}\delta_{jk} + \sum_{j\in J}\sum_{k\in K_j}\sum_{i\in I}(\alpha_i Z_{ijk} + \beta_i Q_{ijk}) + \sum_{w\in\widehat{\Omega}} \widehat{\rho}_w \left(\sum_{j\in J}\sum_{k\in K_j} b_{jk} y_{jkw} + \sum_{i\in I} e_i \phi_{iw} \right), \tag{4.7}$$

subject to Constraints (3.26)–(3.46), with Ω replaced by $\widehat{\Omega}$ in the scenario-dependent constraints.

Model (P4) is solved using CPLEX to obtain the optimal first-stage solution $(\mathbf{h}^\star, \mathbf{p}^\star, \boldsymbol{\delta}^\star, \mathbf{Z}^\star, \mathbf{Q}^\star)$. With the first-stage decisions derived from Model (P4) fixed in Model (P2), the following full-scenario evaluation model is derived:

Model (P5)

$$\min_{\mathbf{y},\boldsymbol{\phi}} \quad \text{Fix} + \sum_{w\in\Omega} r_w \left(\sum_{j\in J}\sum_{k\in K_j} b_{jk} y_{jkw} + \sum_{i\in I} e_i \phi_{iw} \right), \tag{4.8}$$

subject to Constraints (3.26)–(3.46),

where

$$\text{Fix} = \sum_{l\in L}\sum_{j\in J}\sum_{k\in K_j} c_{jkl}h_{jkl} + \sum_{j\in J}\sum_{k\in K_j} v_j p_{jk} + \sum_{j\in J}\sum_{k\in K_j} u_{jk}\delta_{jk} + \sum_{j\in J}\sum_{k\in K_j}\sum_{i\in I}(\alpha_i Z_{ijk} + \beta_i Q_{ijk})$$

denotes the cost determined by the first-stage decisions given by Model (P4) and is therefore treated as a constant in Model (P5). Once the first-stage decisions are fixed, the second-stage decisions are independent across disruption scenarios. Accordingly, Model (P5) can be separated into $|\Omega|$ mutually independent scenario subproblems. The subproblem for disruption scenario w can be formulated as follows:

Model (P5$_s$)

$$\min_{\mathbf{y},\boldsymbol{\phi}} \quad \text{Oper}_w = \sum_{j\in J}\sum_{k\in K_j} b_{jk} y_{jkw} + \sum_{i\in I} e_i \phi_{iw}, \tag{4.9}$$

subject to Constraints (3.26)–(3.46).

By solving Model (P5$_s$) for each scenario in the complete scenario set, the optimal objective value of Model (P5) is obtained as a feasible upper bound for Model (P2):

$$\text{Fix} + \sum_{w\in\Omega} r_w \text{Oper}_w.$$

4.2. Lower-bound computation methods

Although the SR method substantially decreases the number of disruption scenarios and improves computational efficiency, the quality of the resulting upper-bound solution still needs to be evaluated against an effective lower bound. Therefore, two relaxation approaches are introduced to obtain lower bounds for Model (P2) and assess the quality of the upper bound obtained by the SR method. First,

by setting $q_{jkw} = 0$, a bound-relaxed model of Model (P2), denoted by Model (P2v), is obtained as follows:

Model (P2v)

$$\begin{aligned}
\min_{\mathbf{h},\mathbf{p},\boldsymbol{\delta},\mathbf{Z},\mathbf{Q}} \quad & \sum_{l\in L}\sum_{j\in J}\sum_{k\in K_j} c_{jkl}h_{jkl} + \sum_{j\in J}\sum_{k\in K_j} v_j p_{jk} + \sum_{j\in J}\sum_{k\in K_j} u_{jk}\delta_{jk} \\
& + \sum_{j\in J}\sum_{k\in K_j}\sum_{i\in I}(\alpha_i Z_{ijk} + \beta_i Q_{ijk}) + \sum_{w\in\Omega} r_w\left(\sum_{j\in J}\sum_{k\in K_j} b_{jk}y_{jkw} + \sum_{i\in I} e_i\phi_{iw}\right) && (4.10)\\
\text{s.t.} \quad & US_{jk} \geq y_{jkw} - \delta_{jk}, \quad \forall j\in J, k\in K_j, w\in\Omega, && (4.11)\\
& p_{jk}LS_{jk} \leq y_{jkw}, \quad \forall j\in J, k\in K_j, w\in\Omega, && (4.12)
\end{aligned}$$

subject to Constraints (3.26)–(3.35) and (3.38)–(3.46).

Lemma 1. Let $\Delta'(\mathbf{h}', \mathbf{p}', \boldsymbol{\delta}', \mathbf{Z}', \mathbf{Q}')$ and $(\mathbf{h}', \mathbf{p}', \boldsymbol{\delta}', \mathbf{Z}', \mathbf{Q}')$ denote the optimal value and a corresponding optimal solution of Model (P2v), respectively. Then, $\Delta'(\mathbf{h}', \mathbf{p}', \boldsymbol{\delta}', \mathbf{Z}', \mathbf{Q}')$ provides a lower bound for Model (P2).

Proof. Let $\Delta^\star\left(\mathbf{h}^\star, \mathbf{p}^\star, \boldsymbol{\delta}^\star, \mathbf{Z}^\star, \mathbf{Q}^\star\right)$ and $\left(\mathbf{h}^\star, \mathbf{p}^\star, \boldsymbol{\delta}^\star, \mathbf{Z}^\star, \mathbf{Q}^\star\right)$ denote the optimal value and a corresponding optimal solution of Model (P2), respectively. Because Model (P2v) is a mixed-integer linear programming relaxation independent of disruption scenarios, the optimal solution of Model (P2), $\left(\mathbf{h}^\star, \mathbf{p}^\star, \boldsymbol{\delta}^\star, \mathbf{Z}^\star, \mathbf{Q}^\star\right)$, is always feasible for Model (P2v). Therefore,

$$\Delta^\star\left(\mathbf{h}^\star, \mathbf{p}^\star, \boldsymbol{\delta}^\star, \mathbf{Z}^\star, \mathbf{Q}^\star\right) \geq \Delta'(\mathbf{h}', \mathbf{p}', \boldsymbol{\delta}', \mathbf{Z}', \mathbf{Q}').$$

This inequality shows that $\Delta'(\mathbf{h}', \mathbf{p}', \boldsymbol{\delta}', \mathbf{Z}', \mathbf{Q}')$ is a lower bound for Model (P2).

The bound-relaxation method can quickly provide a lower bound for Model (P2), but the global relaxation may yield a relatively weak lower bound. Therefore, the improved SSDDLR method is used to derive a tighter lower bound for Model (P2).

The main computational challenge of Model (P2) arises because the first-stage decision variables $(\mathbf{h}, \mathbf{p}, \boldsymbol{\delta}, \mathbf{Z}, \mathbf{Q})$ are shared across disruption scenarios. Following the DDLR algorithm described by Yin et al. [40], scenario-specific copies of the first-stage decision variables are introduced, allowing Model (P2) to be separated into $|\Omega|$ mutually independent scenario subproblems. Specifically, $(\mathbf{h}_w, \mathbf{p}_w, \boldsymbol{\delta}_w, \mathbf{Z}_w, \mathbf{Q}_w)$, $w = 1, \ldots, |\Omega|$, are introduced, and Model (P2) can be reformulated as follows:

Model (P6)

$$\begin{aligned}
\min_{\substack{\mathbf{h}_w,\mathbf{p}_w,\boldsymbol{\delta}_w,\mathbf{Z}_w,\mathbf{Q}_w;\\ w\in\Omega}} \quad & \sum_{w\in\Omega} r_w\Bigg[\sum_{l\in L}\sum_{j\in J}\sum_{k\in K_j} c_{jkl}h_{jklw} + \sum_{j\in J}\sum_{k\in K_j} v_j p_{jkw} + \sum_{j\in J}\sum_{k\in K_j} u_{jk}\delta_{jkw} \\
& + \sum_{j\in J}\sum_{k\in K_j}\sum_{i\in I}(\alpha_i Z_{ijkw} + \beta_i Q_{ijkw}) + \left(\sum_{j\in J}\sum_{k\in K_j} b_{jk}y_{jkw} + \sum_{i\in I} e_i\phi_{iw}\right)\Bigg]. && (4.13)\\
& (\mathbf{h}_w, \mathbf{p}_w, \boldsymbol{\delta}_w, \mathbf{Z}_w, \mathbf{Q}_w) = (\mathbf{h}_{w+1}, \mathbf{p}_{w+1}, \boldsymbol{\delta}_{w+1}, \mathbf{Z}_{w+1}, \mathbf{Q}_{w+1}), \quad w = 1, \ldots, |\Omega| - 1. && (4.14)\\
& (\mathbf{h}_1, \mathbf{p}_1, \boldsymbol{\delta}_1, \mathbf{Z}_1, \mathbf{Q}_1) = (\mathbf{h}_{|\Omega|}, \mathbf{p}_{|\Omega|}, \boldsymbol{\delta}_{|\Omega|}, \mathbf{Z}_{|\Omega|}, \mathbf{Q}_{|\Omega|}), && (4.15)
\end{aligned}$$

subject to Constraints (3.26)–(3.46).

Constraints (4.14) and (4.15) are nonanticipativity constraints that preserve the equivalence between the decomposed problem and the original problem. Following Yin et al. [40], an auxiliary matrix $\mathbf{G}_w$ formed by identity and zero matrices is introduced to express the nonanticipativity constraints as follows:

$$\sum_{w\in\Omega} \mathbf{G}_w(\mathbf{h}_w^\mathsf{T}, \mathbf{p}_w^\mathsf{T}, \boldsymbol{\delta}_w^\mathsf{T}, \mathbf{Z}_w^\mathsf{T}, \mathbf{Q}_w^\mathsf{T})^\mathsf{T} = 0. \tag{4.16}$$

Let $\boldsymbol{\lambda}$ denote the vector of Lagrangian multipliers. The Lagrangian relaxation (LR) of Model (P6) can then be formulated as follows:

Lagrangian relaxation (LR)

$$\begin{aligned}\min_{\substack{\mathbf{h}_w,\mathbf{p}_w,\boldsymbol{\delta}_w,\mathbf{Z}_w,\mathbf{Q}_w;\\ w\in\Omega}} \quad & \sum_{w\in\Omega} r_w\Bigg[\sum_{l\in L}\sum_{j\in J}\sum_{k\in K_j} c_{jkl}h_{jklw} + \sum_{j\in J}\sum_{k\in K_j} v_j p_{jkw} + \sum_{j\in J}\sum_{k\in K_j} u_{jk}\delta_{jkw} \\ & + \sum_{j\in J}\sum_{k\in K_j}\sum_{i\in I}(\alpha_i Z_{ijkw} + \beta_i Q_{ijkw}) + \left(\sum_{j\in J}\sum_{k\in K_j} b_{jk}y_{jkw} + \sum_{i\in I} e_i\phi_{iw}\right)\Bigg] \\ & + \boldsymbol{\lambda}^\mathsf{T}\sum_{w\in\Omega}\mathbf{G}_w(\mathbf{h}_w^\mathsf{T}, \mathbf{p}_w^\mathsf{T}, \boldsymbol{\delta}_w^\mathsf{T}, \mathbf{Z}_w^\mathsf{T}, \mathbf{Q}_w^\mathsf{T})^\mathsf{T},\end{aligned} \tag{4.17}$$

subject to Constraints (3.26)–(3.46).

The nonanticipativity constraints are relaxed. The LR model can be separated into $|\Omega|$ mutually independent scenario subproblems, thereby enhancing computational efficiency. However, as the disruption-scenario count increases, both the number of subproblems and the size of the auxiliary matrix $\mathbf{G}_w$ increase substantially, raising data loading and storage overhead and reducing the computational efficiency of the DDLR algorithm. To address the resulting computational burden, scenario sorting and contribution-based screening are incorporated into the conventional DDLR algorithm, resulting in the improved SSDDLR method. For each disruption scenario w, let F_w^0 denote the optimal unweighted total cost of its scenario subproblem with the Lagrangian multiplier vector fixed at $\boldsymbol{\lambda} = \mathbf{0}$. This cost includes both first-stage and second-stage costs; the superscript 0 indicates zero multipliers. Unlike Oper_w in Model (P5_s), F_w^0 is not restricted to second-stage recourse costs under fixed first-stage decisions. The probability-weighted scenario contribution is defined as $\text{TC}_w = r_w F_w^0$. All disruption scenarios are then sorted in descending order of TC_w. Let TC^U denote the feasible upper bound obtained through scenario reduction. The relative contribution of scenario w to the upper bound is defined as

$$\sigma_w = \frac{\text{TC}_w}{\text{TC}^U} \times 100\%.$$

Scenarios satisfying $\sigma_w \geq \sigma^\star$ are retained; all remaining scenarios are excluded from the subsequent DDLR procedure. Here, $\sigma^\star$ denotes the scenario-screening threshold and can be adjusted according to the gap between the upper and lower bounds. When the gap is large, reducing $\sigma^\star$ retains more scenarios and improves the accuracy of the lower-bound estimate.

After sorting and screening, the complete scenario set Ω in the LR model is replaced by the retained scenario set $\widetilde{\Omega}$. Accordingly, the subproblem for scenario $\widetilde{w}$ is formulated as follows, where $\widetilde{w} = 1, 2, \ldots, \left|\widetilde{\Omega}\right|$:

Retained-scenario subproblem

$$\begin{aligned}\min_{\mathbf{h}_{\widetilde{w}},\mathbf{p}_{\widetilde{w}},\boldsymbol{\delta}_{\widetilde{w}},\mathbf{Z}_{\widetilde{w}},\mathbf{Q}_{\widetilde{w}}} \quad & r_{\widetilde{w}}\Bigg[\sum_{l\in L}\sum_{j\in J}\sum_{k\in K_j} c_{jkl}h_{jkl\widetilde{w}} + \sum_{j\in J}\sum_{k\in K_j} v_j p_{jk\widetilde{w}} + \sum_{j\in J}\sum_{k\in K_j} u_{jk}\delta_{jk\widetilde{w}} \\ & + \sum_{j\in J}\sum_{k\in K_j}\sum_{i\in I}(\alpha_i Z_{ijk\widetilde{w}} + \beta_i Q_{ijk\widetilde{w}}) + \left(\sum_{j\in J}\sum_{k\in K_j} b_{jk}y_{jk\widetilde{w}} + \sum_{i\in I} e_i\phi_{i\widetilde{w}}\right)\Bigg] \\ & + \boldsymbol{\lambda}^{\mathsf{T}}\mathbf{G}_{\widetilde{w}}(\mathbf{h}_{\widetilde{w}}^{\mathsf{T}}, \mathbf{p}_{\widetilde{w}}^{\mathsf{T}}, \boldsymbol{\delta}_{\widetilde{w}}^{\mathsf{T}}, \mathbf{Z}_{\widetilde{w}}^{\mathsf{T}}, \mathbf{Q}_{\widetilde{w}}^{\mathsf{T}})^{\mathsf{T}}, \end{aligned} \tag{4.18}$$

subject to Constraints (3.26)–(3.46).

Let LD represent the optimal value of the corresponding Lagrangian dual problem, which can be formulated as follows:

$$\mathrm{LD} = \max_{\boldsymbol{\lambda}} \mathrm{LR}(\boldsymbol{\lambda}). \tag{4.19}$$

Following Yin et al. [40], the Lagrangian dual problem can be solved using a subgradient method. In the subgradient method,

$$\sum_{\widetilde{w}\in\widetilde{\Omega}} \mathbf{G}_{\widetilde{w}}\left(((\mathbf{h}^{\star})_{\widetilde{w}})^{\mathsf{T}}, ((\mathbf{p}^{\star})_{\widetilde{w}})^{\mathsf{T}}, ((\boldsymbol{\delta}^{\star})_{\widetilde{w}})^{\mathsf{T}}, ((\mathbf{Z}^{\star})_{\widetilde{w}})^{\mathsf{T}}, ((\mathbf{Q}^{\star})_{\widetilde{w}})^{\mathsf{T}}\right)^{\mathsf{T}}$$

constitutes a subgradient of the Lagrangian dual problem. Accordingly, the subgradient algorithm is designed as follows:

Algorithm 2. Subgradient procedure

Step 1. Initialization. Initialize the Lagrangian multiplier vector $\boldsymbol{\lambda}^1$, and set $k = 1$.

Step 2. Subproblem solution and bound update. Given $\boldsymbol{\lambda}^k$, solve the $|\widetilde{\Omega}|$ independent subproblems, and compute the corresponding subgradient

$$\sum_{\widetilde{w}\in\widetilde{\Omega}} \mathbf{G}_{\widetilde{w}}\left(((\mathbf{h}^{\star})_{\widetilde{w}})^{\mathsf{T}}, ((\mathbf{p}^{\star})_{\widetilde{w}})^{\mathsf{T}}, ((\boldsymbol{\delta}^{\star})_{\widetilde{w}})^{\mathsf{T}}, ((\mathbf{Z}^{\star})_{\widetilde{w}})^{\mathsf{T}}, ((\mathbf{Q}^{\star})_{\widetilde{w}})^{\mathsf{T}}\right)^{\mathsf{T}}.$$

Then, calculate the current objective value of the Lagrangian dual problem, and store the best value obtained up to iteration k as $\Phi^{\star}$.

Step 3. Multiplier update and termination test. Update the Lagrangian multipliers as follows:

$$\boldsymbol{\lambda}^{k+1} = \boldsymbol{\lambda}^k + s^k \sum_{\widetilde{w}\in\widetilde{\Omega}} \mathbf{G}_{\widetilde{w}}\left(((\mathbf{h}^{\star})_{\widetilde{w}})^{\mathsf{T}}, ((\mathbf{p}^{\star})_{\widetilde{w}})^{\mathsf{T}}, ((\boldsymbol{\delta}^{\star})_{\widetilde{w}})^{\mathsf{T}}, ((\mathbf{Z}^{\star})_{\widetilde{w}})^{\mathsf{T}}, ((\mathbf{Q}^{\star})_{\widetilde{w}})^{\mathsf{T}}\right)^{\mathsf{T}}. \tag{4.20}$$

Following Yin et al. [40], the step size and the associated parameters are defined as follows:

$$\begin{aligned} s^k &= \alpha^k \frac{\beta^k - \mathrm{LR}(\boldsymbol{\lambda}^k)}{\left\| \sum_{\widetilde{w} \in \widetilde{\Omega}} \mathbf{G}_{\widetilde{w}} \left(((\mathbf{h}^\star)_{\widetilde{w}})^\mathsf{T}, ((\mathbf{p}^\star)_{\widetilde{w}})^\mathsf{T}, ((\boldsymbol{\delta}^\star)_{\widetilde{w}})^\mathsf{T}, ((\mathbf{Z}^\star)_{\widetilde{w}})^\mathsf{T}, ((\mathbf{Q}^\star)_{\widetilde{w}})^\mathsf{T} \right)^\mathsf{T} \right\|^2}, \\ \alpha^k &= \kappa(k), \\ \beta^k &= (1 + \kappa'(k))\Phi^\star, \end{aligned} \tag{4.21}$$

where $\Phi^\star$ denotes the best objective value obtained up to iteration k, and $\kappa(k)$ and $\kappa'(k)$ are positive linear functions that decrease monotonically with k. The termination criterion is defined as

$$\left| \frac{\mathrm{LR}(\boldsymbol{\lambda}^{k+1}) - \mathrm{LR}(\boldsymbol{\lambda}^k)}{\mathrm{LR}(\boldsymbol{\lambda}^k)} \right| \leq \varepsilon. \tag{4.22}$$

Here, ε is a prespecified maximum tolerance. If the termination criterion in (4.22) is satisfied, the procedure terminates; otherwise, the Lagrangian multipliers are updated, and a new objective value is calculated.

By duality,

$$\Phi^\star + \sum_{w \in \Omega \setminus \widetilde{\Omega}} \mathrm{TC}_w^\star$$

provides a lower bound for Model (P2) and because Models (P1) and (P2) are equivalent, also for the original stochastic model. Here, $\mathrm{TC}_w^\star$ denotes the objective value of the subproblem corresponding to scenario $w \in \Omega \setminus \widetilde{\Omega}$, obtained by fixing the Lagrangian multiplier vector $\boldsymbol{\lambda}$ at zero.

5. Numerical experiments

Numerical experiments based on an African container-shipping network are conducted to examine the computational performance of the proposed algorithm, the effects of key parameters on procurement decisions, and the performance of alternative resilience strategies. All experiments were conducted using IBM ILOG CPLEX Optimization Studio 22.1.1. The proposed algorithm and the initial direct-solution experiments were run on a computer equipped with an AMD Ryzen 7 5800H processor and 16 GB of RAM. Supplementary direct-solution experiments were conducted on a computer equipped with an Intel Core i9-14900 processor and 64 GB of RAM.

Section 5.1 describes the case data and parameter settings. Section 5.2 compares the computational results of SR-SSDDLR with those obtained by directly solving the model using CPLEX. Section 5.3 examines the effects of key parameters, Section 5.4 compares resilience strategies, and Section 5.5 discusses managerial implications.

5.1. Case data and parameter settings

The experimental case is constructed from the liner-shipping benchmark data of Brouer et al. [41] and comprises 29 transportation tasks and 42 candidate 3PLs. The candidate 3PLs offer transportation services through bundle bids, from which the 4PL selects winning bids and determines the allocated transportation volumes. Parameter settings associated with the WD mechanism and disruption scenarios follow the setting methods of Qian et al. [21], with specific values selected for the present case. Parameters associated with multilevel fortification and soft time windows are specified for the model considered here, and the investment budget, unit emergency outsourcing cost, carbon emission cap, and time windows are varied according to the experimental design. Table 3 summarizes the parameter values and setting rules, with units specified in the notes.

Table 3. Parameter settings for the numerical experiments.

Parameter	Value	Parameter	Value
$\|I\|$	29	$\|J\|$	42
$\max_j \|K_j\|$	5	Active bundle bids	124
$N_{\min}$	5	$N_{\max}$	37
d_i	186–6000	v_j	2012–4293
b_{jk}	50–1632	u_{jk}	10–49
US_{jk}	50–2920	LS_{jk}	$0.1US_{jk}$
A_{jk}	50–89	t_{ijk}	10–43
α_i	104–297	β_i	101–271
CE_{jk}	17.28–65.98	CE_i^O	39.60–46.60
		B	10^7
$C_{\max}$	1000; 5000; 10,000; 30,000; 50,000		
Cap	300,000; 350,000; 400,000; 450,000; 500,000; 700,000		
$e_i = e$	100; 150; 200; 300; 500; 1000		
$[T_{\min,i}, T_{\max,i}]$	$[0, 48]$; $[12, 36]$; $[24, 36]$; $[36, 48]$		
a_{ijk}	{0, 1}, specified by bid coverage		
q_{jkw}	{0, 1}, specified by disruption states		
r_w	Product of event-state probabilities		
Number of scenarios before reduction	1024		
Number of scenarios after reduction	5		
Reduced probabilities	0.50; 0.20; 0.15; 0.10; 0.05		
Fortification level l	1	2	3
c_{jkl}	0	2804–3100	5805–6100
ψ_{jkl}	0	0.40–0.60	1

Notes: Time and costs are expressed in h and USD, respectively; unit prices and time penalties are in USD/TEU and USD/h. Transportation volumes are measured in TEU. Emission factors are expressed in kg CO_2e/TEU, and the carbon-emission cap is measured in kg CO_2e. The table summarizes the parameter values used across the experiments; the specific combinations are described in the corresponding experimental subsections.

5.2. Algorithm performance evaluation

To evaluate the computational performance of SR-SSDDLR under large-scale disruption scenarios, the algorithm results are compared with those obtained by directly solving Model (P2) using CPLEX in the 16GB and 64GB environments, as shown in Table 4. No time limit was imposed on the original 16GB experiments. A time limit of 3600 s was imposed for the supplementary 64GB experiments. The reported 16GB runs terminated because of insufficient memory; the corresponding objective values and gaps are reported as NA, together with the elapsed times from launch to the memory errors. The objective value reported for SR-SSDDLR is the total cost of the obtained feasible solution evaluated over the full set of 1024 scenarios and provides an upper bound on the optimal value of the original problem. Total computation time includes reduced-scenario optimization, full-scenario evaluation, and lower-bound computation.

Table 4. Computational results of SR-SSDDLR and CPLEX under different protective investment budgets and unit emergency outsourcing costs.

		SR-SSDDLR				CPLEX (16GB)			CPLEX (64GB; 3600 s limit)	
$C_{\max}$	e	Objective value (upper bound)	Lower bound	Total time (s)	Gap (%)	Objective value	Time to error (s)	Gap (%)	Objective value	Gap (%)
30,000	100	1,529,646.00	1,522,840.79	53.08	0.44	NA	420.17	NA	1,843,349.27	17.10
	150	1,594,840.49	1,578,053.68	63.10	1.05	NA	356.96	NA	2,419,406.83	36.14
	200	1,620,841.49	1,600,025.78	106.34	1.28	NA	154.38	NA	2,995,464.39	47.76
	300	1,649,734.18	1,620,564.51	164.58	1.77	NA	258.93	NA	4,147,579.51	62.11
	500	1,675,186.65	1,643,445.35	158.17	1.89	NA	500.64	NA	6,451,809.76	100.00
50,000	100	1,529,646.00	1,522,817.31	64.71	0.45	NA	403.28	NA	1,532,990.60	0.48
	150	1,594,150.92	1,578,088.45	72.56	1.01	NA	436.75	NA	2,247,383.87	31.25
	200	1,617,069.56	1,600,016.94	97.95	1.05	NA	146.52	NA	2,674,865.38	41.50
	300	1,642,576.00	1,620,579.52	147.09	1.34	NA	478.00	NA	3,529,828.39	55.48
	500	1,666,721.00	1,643,450.87	184.52	1.40	NA	149.92	NA	5,239,754.40	100.00

As shown in Table 4, SR-SSDDLR obtains feasible solutions for all ten parameter combinations, with total computation times of 53.08–184.52 s, including reduced-scenario optimization, full-scenario evaluation, and lower-bound computation. In contrast, all direct CPLEX runs in the 16GB environment terminate because of insufficient memory. After increasing the memory to 64GB and imposing a time limit of 3600 s, the objective values obtained by CPLEX remain higher than those obtained by SR-SSDDLR for all ten parameter combinations. Moreover, the relative gaps between the feasible objective values and lower bounds of SR-SSDDLR range from 0.44% to 1.89%, indicating small optimality gaps. These results demonstrate that for the tested large-scale liner shipping instances, SR-SSDDLR obtains near-optimal feasible solutions within short computation times, showing advantages in computational efficiency and solution quality.

5.3. Parameter sensitivity analysis

This section examines the effects of the unit emergency outsourcing cost e, protective investment budget $C_{\max}$, and carbon-emission cap on procurement costs and resilience strategy configuration under different soft time windows. For clarity, the following symbols are used: TC for total procurement cost, W_1 for total emergency outsourcing cost, W_2 for soft time-window penalty cost, W_3 for actual protective investment cost, J_G for the number of fortified bundle bids, and Y_L for the number of bundle bids with reserved capacity.

5.3.1. Effects of outsourcing cost on solution outcomes

To examine the effects of the unit emergency outsourcing cost e, the protective investment budget $C_{\max}$ is set to USD 50,000, and four soft time-window settings are considered: $T \in \{[0, 48], [12, 36], [24, 36], [36, 48]\}$, where $T = [T_{\min}, T_{\max}]$ denotes the common soft-time window for all transportation tasks. Table 5 and Figure 5 report the total procurement cost (TC), total emergency outsourcing cost (W_1), number of fortified bundle bids (J_G), and number of bundle bids with reserved capacity (Y_L) under the different settings.

Table 5. Experimental results under different values of e and soft time-window settings.

T	Measure	Unit emergency outsourcing cost e				
		100	150	300	500	1000
0–48	TC	1,519,015.00	1,580,719.43	1,625,610.00	1,643,562.00	1,650,191.40
	W_1	220,700.00	84,250.48	45,300.00	13,500.00	0.00
	J_G	1	3	3	4	4
	Y_L	13	16	16	13	14
12–36	TC	1,529,646.00	1,594,150.92	1,642,576.00	1,666,721.00	1,676,698.40
	W_1	261,500.00	104,332.69	45,300.00	13,500.00	0.00
	J_G	1	3	3	4	4
	Y_L	11	15	16	14	14
24–36	TC	1,564,110.00	1,638,037.20	1,694,692.00	1,727,494.00	1,743,462.00
	W_1	254,100.00	104,332.69	63,000.00	54,250.00	27,000.00
	J_G	1	3	3	4	4
	Y_L	12	15	13	16	13
36–48	TC	1,624,169.00	1,716,696.00	1,800,184.78	1,845,839.00	1,864,099.00
	W_1	452,700.00	148,200.00	103,473.08	99,000.00	27,000.00
	J_G	1	2	3	3	4
	Y_L	12	16	14	15	13

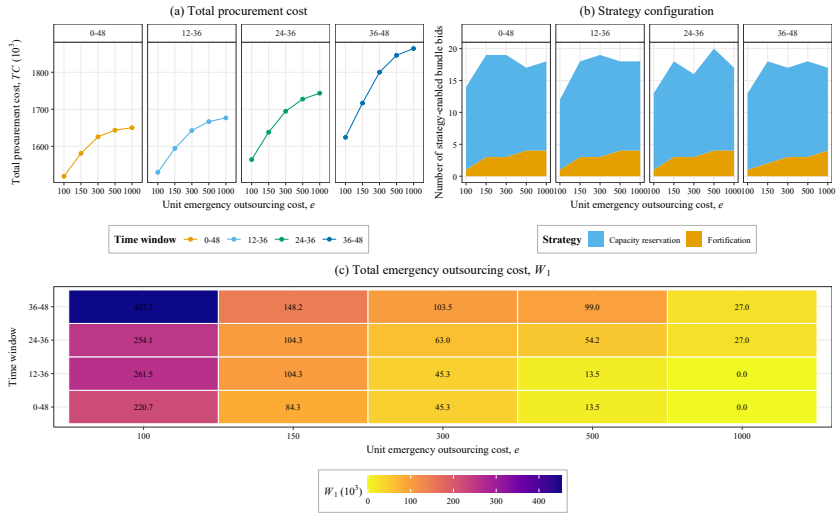


Figure 5. Effects of the unit emergency outsourcing cost on optimal decisions.

As shown by the total cost curves in Figure 5(a), TC increases monotonically with the unit emergency outsourcing cost e under all time window settings. At the same value of e, a tighter time window results in a higher total procurement cost, indicating a positive relationship between the stringency of timeliness requirements and overall procurement cost. Under $T = [36, 48]$, increasing e from 100 to 1000 raises TC by 14.8%, whereas under $T = [0, 48]$, the corresponding increase is only 8.6%. The smaller increase under $T = [0, 48]$ indicates that a looser time window reduces the sensitivity of total procurement cost to the unit emergency outsourcing cost.

Figure 5(b) indicates that the unit emergency outsourcing cost e is linked to the deployment intensity of fortification and capacity reservation. As e increases, the number of fortified bundle bids (J_G) gradually rises from 1 to 4, whereas the number of bundle bids with reserved capacity (Y_L) varies across the tested settings. At lower levels of e, the 4PL relies more heavily on emergency outsourcing. As emergency outsourcing becomes more costly, greater investment is allocated to fortification and capacity reservation, shifting the resilience strategy from postdisruption emergency response toward a greater use of predisruption resilience measures.

As shown by the heatmap of total emergency outsourcing cost in Figure 5(c), W_1 decreases continuously as the unit emergency outsourcing cost e increases. At a given unit emergency outsourcing cost, total emergency outsourcing cost varies with the time-window requirements. When $e = 100$, and $T = [36, 48]$, W_1 reaches the maximum value of 452,700. When $e = 1000$, W_1 falls to relatively low levels across all time window settings and approaches zero in some cases. The decline in W_1 as e increases indicates that higher values of the unit emergency outsourcing cost encourage the 4PL to strengthen internal risk mitigation and reduce reliance on emergency outsourcing.

Overall, as e increases, total procurement cost rises, but reliance on emergency outsourcing declines. Fortification is used more frequently, and capacity reservation remains widely adopted, indicating greater use of predisruption resilience measures. In particular, the noticeable increase in the number of fortified bundle bids as e ranges from 300 to 500 suggests a shift away from reliance on postdisruption emergency outsourcing.

5.3.2. Effects of the protective investment budget on solution outcomes

Section 5.3.1 examines the unit emergency outsourcing cost at a protective investment budget of 50,000. To further examine the effects of the protective investment budget $C_{\max}$, five budget levels are considered: 1000, 5000, 10,000, 30,000, and 50,000. Experiments are conducted under four soft time-window settings—0–48, 12–36, 24–36, and 36–48—to analyze the effects of budget changes on total procurement cost (TC), total emergency outsourcing cost (W_1), soft time-window penalty cost (W_2), actual protective investment cost (W_3), the number of fortified bundle bids (J_G), and the number of bundle bids with reserved capacity (Y_L). The results are reported in Table 6 and Figures 6 and 7.

Table 6. Experimental results under different values of $C_{\max}$ and soft time-window settings.

T	e	Measure	$C_{\max}$				
			1000	5000	10,000	30,000	50,000
0–48	$e = 100$	TC	1,564,147.89	1,548,625.43	1,535,798.49	1,519,052.84	1,519,015.00
0–48	$e = 100$	W_1	291,110.53	292,840.00	261,865.48	219,747.37	220,700.00
0–48	$e = 100$	W_2	0.00	0.00	0.00	0.00	0.00
0–48	$e = 100$	W_3	1000.00	5000.00	10,000.00	30,000.00	30,253.00
0–48	$e = 100$	J_G	0	1	1	1	1
0–48	$e = 100$	Y_L	1	2	7	13	13

Table 6. Experimental results under different values of $C_{\max}$ and soft time-window settings (continued).

T	e	Measure	$C_{\max}$				
			1000	5000	10,000	30,000	50,000
0–48	e = 150	TC	1,662,111.66	1,640,801.96	1,619,792.57	1,581,581.49	1,580,719.43
0–48	e = 150	W_1	197,755.74	146,562.00	139,829.81	97,518.77	84,250.48
0–48	e = 150	W_2	0.00	0.00	0.00	0.00	0.00
0–48	e = 150	W_3	1000.00	5000.00	10,000.00	30,000.00	33,439.03
0–48	e = 150	J_G	0	0	2	3	3
0–48	e = 150	Y_L	3	4	4	13	16
0–48	e = 300	TC	1,777,875.58	1,718,884.70	1,666,275.54	1,631,337.85	1,625,610.00
0–48	e = 300	W_1	186,258.64	120,405.00	61,586.47	52,490.17	45,300.00
0–48	e = 300	W_2	0.00	0.00	0.00	0.00	0.00
0–48	e = 300	W_3	1000.00	5000.00	10,000.00	25,213.89	37,751.00
0–48	e = 300	J_G	0	0	1	2	3
0–48	e = 300	Y_L	2	6	7	12	16
0–48	e = 500	TC	1,889,586.25	1,793,109.39	1,703,247.42	1,654,284.87	1,643,562.00
0–48	e = 500	W_1	266,950.00	174,280.00	92,193.39	34,333.33	13,500.00
0–48	e = 500	W_2	0.00	0.00	0.00	0.00	0.00
0–48	e = 500	W_3	1000.00	5000.00	10,000.00	29,488.54	41,558.00
0–48	e = 500	J_G	0	0	1	3	4
0–48	e = 500	Y_L	3	5	6	14	13
0–48	e = 1000	TC	2,088,565.31	1,890,183.19	1,767,191.00	1,665,799.10	1,650,191.40
0–48	e = 1000	W_1	389,054.76	187,885.79	68,089.29	4666.67	0.00
0–48	e = 1000	W_2	0.00	0.00	0.00	0.00	0.00
0–48	e = 1000	W_3	1000.00	5000.00	10,000.00	29,477.10	38,298.40
0–48	e = 1000	J_G	0	0	0	3	4
0–48	e = 1000	Y_L	4	5	11	14	14
12–36	e = 100	TC	1,579,961.56	1,563,303.43	1,547,866.32	1,529,646.00	1,529,646.00
12–36	e = 100	W_1	303,122.22	315,540.00	272,081.82	261,500.00	261,500.00
12–36	e = 100	W_2	14,515.00	13,279.00	8943.00	8763.00	8763.00
12–36	e = 100	W_3	1000.00	5000.00	10,000.00	26,147.00	26,147.00
12–36	e = 100	J_G	0	1	1	1	1
12–36	e = 100	Y_L	2	2	6	11	11
12–36	e = 150	TC	1,679,827.21	1,658,582.40	1,636,316.33	1,594,840.49	1,594,150.92
12–36	e = 150	W_1	200,985.31	201,645.00	148,143.50	97,518.77	104,332.69
12–36	e = 150	W_2	16,629.00	15,523.00	16,228.00	13,259.00	12,590.00
12–36	e = 150	W_3	1000.00	5000.00	10,000.00	30,000.00	32,131.12
12–36	e = 150	J_G	0	0	2	3	3
12–36	e = 150	Y_L	2	5	4	13	15
12–36	e = 300	TC	1,806,107.70	1,745,892.62	1,691,390.84	1,649,734.18	1,642,576.00
12–36	e = 300	W_1	185,715.00	122,259.48	61,742.36	67,500.00	45,300.00
12–36	e = 300	W_2	28,090.00	24,119.00	22,460.00	14,958.00	16,966.00
12–36	e = 300	W_3	1000.00	5000.00	10,000.00	30,000.00	37,751.00
12–36	e = 300	J_G	0	0	1	3	3
12–36	e = 300	Y_L	3	3	8	14	16
12–36	e = 500	TC	1,917,869.25	1,821,673.39	1,729,217.42	1,675,186.65	1,666,721.00
12–36	e = 500	W_1	266,950.00	174,280.00	92,193.39	35,000.00	13,500.00
12–36	e = 500	W_2	28,283.00	28,564.00	25,970.00	20,435.00	23,159.00
12–36	e = 500	W_3	1000.00	5000.00	10,000.00	30,000.00	42,422.00
12–36	e = 500	J_G	0	0	1	2	4
12–36	e = 500	Y_L	3	5	6	17	14
12–36	e = 1000	TC	2,117,030.31	1,922,922.19	1,795,664.19	1,689,104.10	1,676,698.40
12–36	e = 1000	W_1	389,054.76	187,885.79	81,000.00	4666.67	0.00
12–36	e = 1000	W_2	28,465.00	32,739.00	24,259.00	23,305.00	26,507.00
12–36	e = 1000	W_3	1000.00	5000.00	10,000.00	29,477.10	38,298.40
12–36	e = 1000	J_G	0	0	1	3	4
12–36	e = 1000	Y_L	4	5	10	14	14
24–36	e = 100	TC	1,618,533.16	1,601,505.92	1,584,224.23	1,564,110.00	1,564,110.00
24–36	e = 100	W_1	428,747.37	413,082.76	325,100.00	254,100.00	254,100.00
24–36	e = 100	W_2	39,184.00	38,440.00	41,809.00	38,211.00	38,211.00
24–36	e = 100	W_3	1000.00	5000.00	10,000.00	28,595.00	28,595.00
24–36	e = 100	J_G	0	1	1	1	1
24–36	e = 100	Y_L	1	2	6	12	12

Table 6. Experimental results under different values of $C_{\max}$ and soft time-window settings (continued).

T	e	Measure	$C_{\max}$				
			1000	5000	10,000	30,000	50,000
24–36	e = 150	TC	1,740,644.16	1,708,957.69	1,682,498.18	1,638,116.00	1,638,037.20
24–36	e = 150	W_1	214,365.79	212,414.79	184,089.33	113,550.00	104,332.69
24–36	e = 150	W_2	68,287.00	63,702.00	61,442.00	45,117.00	54,650.00
24–36	e = 150	W_3	1000.00	5000.00	10,000.00	29,432.00	32,131.12
24–36	e = 150	J_G	0	0	2	2	3
24–36	e = 150	Y_L	1	3	4	10	15
24–36	e = 300	TC	1,882,857.58	1,815,739.76	1,752,838.89	1,705,024.00	1,694,692.00
24–36	e = 300	W_1	186,258.64	146,196.00	82,888.04	96,600.00	63,000.00
24–36	e = 300	W_2	104,982.00	86,489.00	76,611.00	55,817.00	64,649.00
24–36	e = 300	W_3	1000.00	5000.00	10,000.00	30,000.00	36,420.00
24–36	e = 300	J_G	0	0	1	2	3
24–36	e = 300	Y_L	2	5	6	13	13
24–36	e = 500	TC	2,006,841.85	1,898,341.91	1,799,197.42	1,735,438.21	1,727,494.00
24–36	e = 500	W_1	309,941.07	199,364.29	92,193.39	51,000.00	54,250.00
24–36	e = 500	W_2	104,982.00	89,326.00	95,950.00	73,013.00	73,553.00
24–36	e = 500	W_3	1000.00	5000.00	10,000.00	28,179.21	43,152.00
24–36	e = 500	J_G	0	0	1	3	4
24–36	e = 500	Y_L	2	6	6	14	16
24–36	e = 1000	TC	2,225,647.31	2,022,722.12	1,886,001.00	1,763,362.72	1,743,462.00
24–36	e = 1000	W_1	389,054.76	198,042.05	95,669.12	28,000.00	27,000.00
24–36	e = 1000	W_2	137,082.00	128,815.00	105,394.00	88,131.00	86,400.00
24–36	e = 1000	W_3	1000.00	5000.00	10,000.00	29,971.67	41,558.00
24–36	e = 1000	J_G	0	0	1	2	4
24–36	e = 1000	Y_L	4	5	7	17	13
36–48	e = 100	TC	1,678,839.16	1,660,028.07	1,643,411.38	1,624,169.00	1,624,169.00
36–48	e = 100	W_1	603,447.37	577,782.76	515,637.50	452,700.00	452,700.00
36–48	e = 100	W_2	69,627.00	65,694.00	65,694.00	77,078.00	77,078.00
36–48	e = 100	W_3	1000.00	5000.00	10,000.00	28,286.00	28,286.00
36–48	e = 100	J_G	0	1	1	1	1
36–48	e = 100	Y_L	1	4	6	12	12
36–48	e = 150	TC	1,842,114.00	1,804,829.38	1,775,598.97	1,720,942.12	1,716,696.00
36–48	e = 150	W_1	314,534.21	268,303.45	277,832.43	149,803.12	148,200.00
36–48	e = 150	W_2	138,281.00	127,952.00	126,730.00	120,982.00	111,983.00
36–48	e = 150	W_3	1000.00	5000.00	10,000.00	30,000.00	39,124.00
36–48	e = 150	J_G	0	0	0	2	2
36–48	e = 150	Y_L	2	6	10	12	16
36–48	e = 300	TC	2,011,616.42	1,934,139.99	1,860,878.90	1,810,967.00	1,800,184.78
36–48	e = 300	W_1	241,057.89	175,643.75	91,986.64	110,400.00	103,473.08
36–48	e = 300	W_2	196,899.00	178,523.00	182,214.00	153,215.00	149,730.00
36–48	e = 300	W_3	1000.00	5000.00	10,000.00	29,909.00	36,030.45
36–48	e = 300	J_G	0	0	1	2	3
36–48	e = 300	Y_L	2	8	6	14	14
36–48	e = 500	TC	2,159,722.85	2,030,740.50	1,920,984.31	1,858,501.87	1,845,839.00
36–48	e = 500	W_1	309,941.07	178,575.00	130,556.05	70,500.00	99,000.00
36–48	e = 500	W_2	257,863.00	228,229.00	195,189.00	167,281.00	162,271.00
36–48	e = 500	W_3	1000.00	5000.00	10,000.00	30,000.00	38,611.00
36–48	e = 500	J_G	0	0	1	2	3
36–48	e = 500	Y_L	2	5	7	17	15
36–48	e = 1000	TC	2,428,060.67	2,178,233.63	2,028,774.80	1,900,246.00	1,864,099.00
36–48	e = 1000	W_1	479,300.00	242,113.24	166,309.16	32,000.00	27,000.00
36–48	e = 1000	W_2	269,061.00	251,313.00	227,445.00	196,206.00	204,806.00
36–48	e = 1000	W_3	1000.00	5000.00	10,000.00	20,805.00	41,558.00
36–48	e = 1000	J_G	0	0	1	1	4
36–48	e = 1000	Y_L	4	5	7	13	13

As shown in Figure 6(a), the total procurement cost (TC) decreases as the protective investment budget $C_{\max}$ increases. When $C_{\max}$ increases from 1000 to 30,000, TC decreases across all tested settings, with reductions ranging from approximately 2.9% to 21.7%. Further increasing the budget to 50,000 yields only limited additional reductions, below 2% in all tested cases, indicating diminishing marginal returns to protective investment.

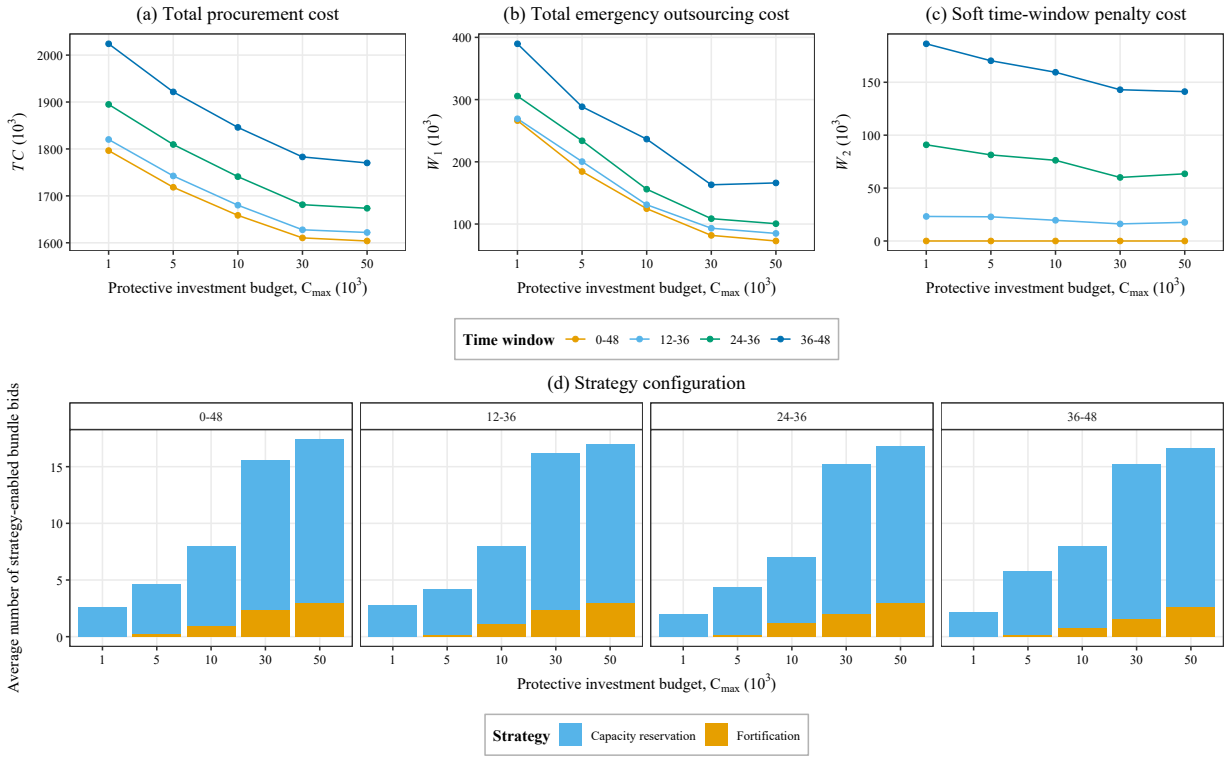


Figure 6. Effects of the protective investment budget on costs and resilience strategy configuration. Values in panels (a)–(d) are averaged over the five tested unit emergency outsourcing cost levels for each combination of $C_{\max}$ and soft time-window setting.

Figure 6(b) indicates an overall decline in total emergency outsourcing cost (W_1) as the protective investment budget increases, with a more pronounced reduction under tighter time-window settings. Under low-budget conditions, insufficient resources are available for fortification and capacity reservation, resulting in greater reliance on costly emergency outsourcing. As the budget increases, internal risk mitigation capacity is strengthened, and the demand for emergency outsourcing declines substantially.

Figure 6(c) indicates that the soft time-window penalty cost (W_2) is primarily determined by the tightness of the time window. Under loose time-window settings, W_2 remains close to zero or at a relatively low level, whereas tighter time windows generally result in higher W_2. As the protective investment budget increases, W_2 varies across the tested settings rather than following a consistent upward or downward trend. This response suggests that protective investment affects timeliness penalties mainly indirectly by improving available transportation capacity and reducing reliance on emergency outsourcing; the effect on W_2 depends on the unit emergency outsourcing cost and the task allocation structure.

Figure 6(d) illustrates the configuration patterns of fortification and capacity reservation under different levels of $C_{\max}$. The results reveal a clear shift in strategy preference as the protective investment budget increases. Under low-budget conditions, capacity reservation is favored to provide flexible capacity support against potential disruptions. As the budget increases, the number of fortified bundle bids rises markedly, whereas capacity reservation remains widely adopted. The increasing use of fortification at higher budget levels indicates that greater protective investment

strengthens predisruption resilience, shifting the response from reactive emergency measures toward proactive protection.

Overall, increasing the protective investment budget reduces total procurement cost and reliance on emergency outsourcing while gradually shifting the resilience strategy from a capacity-reservation-dominated configuration under low budgets toward a coordinated use of fortification and capacity reservation. However, the cost-reduction benefits diminish markedly as the budget continues to increase, indicating clear diminishing marginal returns to protective investment.

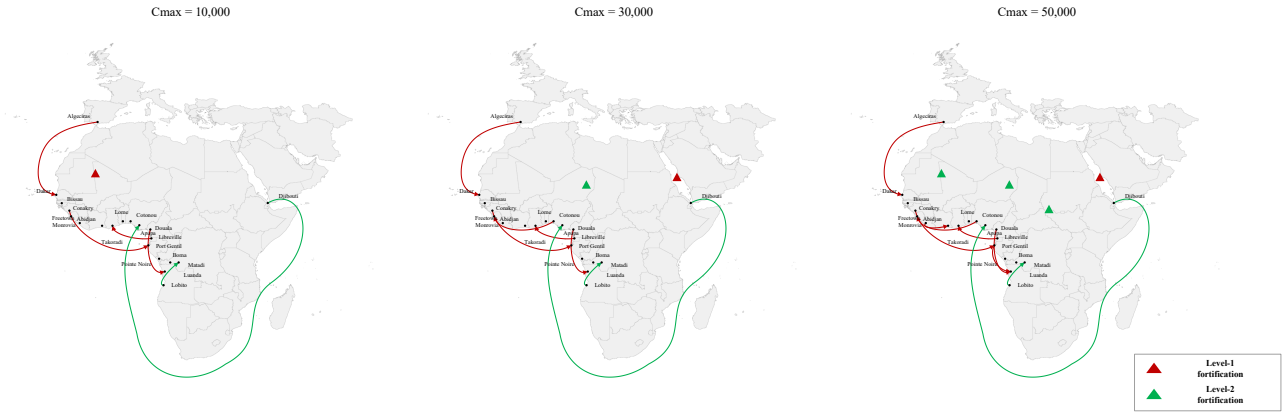


Figure 7. Schematic illustration of fortification decisions under different protective investment budgets.

Figure 7 provides a schematic illustration of the fortification decisions at $C_{\max} = 10,000$, 30,000, and 50,000, with $e = 500$ and a soft time window of 12–36 h. The numbers of fortified bundle bids are 1, 2, and 4, respectively. At a budget of 10,000, one bid receives level-1 fortification; at 30,000, one bid receives level-1 and one receives level-2 fortification; at 50,000, one bid receives level-1 and three receive level-2 fortification. The two plotted levels denote the two positive-investment fortification options. The curves indicate illustrative service connections, and triangle positions are schematic markers for fortified bids.

5.3.3. Effects of the carbon emission cap under different time windows

To examine the combined effects of carbon restrictions and time-window requirements on procurement decisions, the carbon-emission cap is set to 300,000, 350,000, 400,000, 450,000, and 500,000 under four time-window settings: 0–48, 12–36, 24–36, and 36–48. The protective investment budget $C_{\max} = 50,000$ and unit emergency outsourcing cost $e = 100$ are fixed, and all other parameters remain unchanged. Table 7 reports emissions and resilience decisions under all four time-window settings, and Figure 8 presents total procurement cost and expected emergency outsourcing volume under all four time-window settings.

Table 7. Emissions and resilience decisions under different carbon-emission caps and time windows.

T	Carbon cap	Maximum scenario emissions	Fortified bids at levels 1/2/3	Total reserved capacity	Expected outsourcing volume
0–48	500,000	449,466.47	0 / 0 / 1	719.00	2207.00
	450,000	449,466.47	0 / 0 / 1	719.00	2207.00
	400,000	400,000.00	0 / 1 / 1	581.17	1479.05
	350,000	350,000.00	0 / 3 / 0	476.31	1278.00
	300,000	300,000.00	0 / 2 / 2	743.76	820.50
12–36	500,000	452,610.64	0 / 0 / 1	606.00	2615.00
	450,000	450,000.00	0 / 0 / 1	606.00	2549.83
	400,000	400,000.00	0 / 0 / 2	527.00	1594.00
	350,000	350,000.00	0 / 3 / 0	511.17	1474.21
	300,000	300,000.00	0 / 2 / 2	761.43	894.50
24–36	500,000	482,663.75	0 / 0 / 1	683.00	2541.00
	450,000	450,000.00	0 / 0 / 1	680.00	2206.00
	400,000	400,000.00	0 / 0 / 2	553.00	1957.00
	350,000	350,000.00	0 / 3 / 0	459.44	1141.94
	300,000	300,000.00	0 / 0 / 2	723.42	967.86
36–48	500,000	500,000.00	0 / 0 / 1	761.34	3238.66
	450,000	450,000.00	0 / 0 / 2	570.00	2975.00
	400,000	400,000.00	0 / 1 / 1	604.00	2448.00
	350,000	350,000.00	0 / 1 / 1	643.00	1080.00
	300,000	300,000.00	0 / 1 / 1	692.14	1100.22

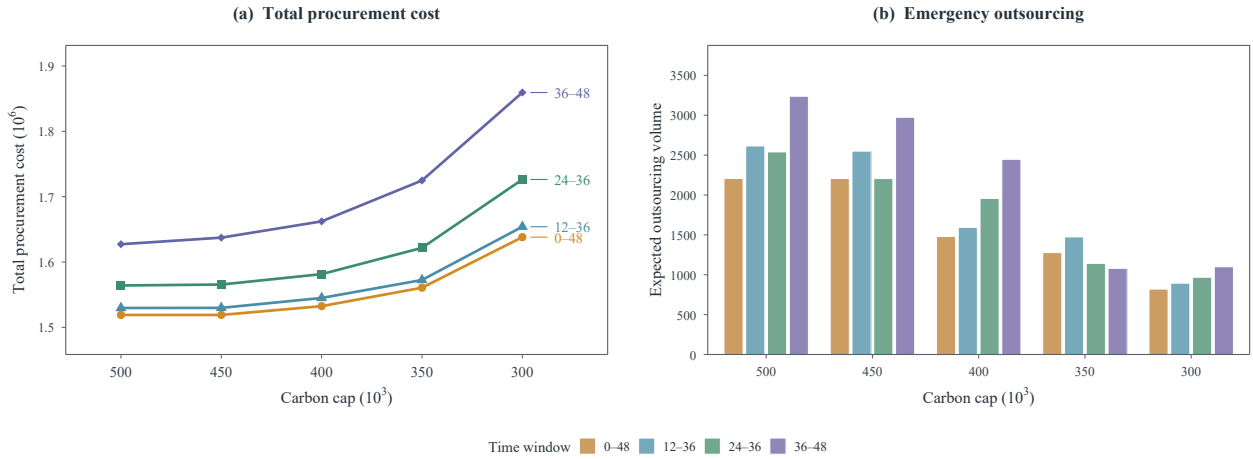


Figure 8. Total procurement cost and expected emergency outsourcing volume under different carbon-emission caps and time windows.

As shown in Figure 8(a), tightening the carbon-emission cap increases the total procurement cost. Reducing the cap from 500,000 to 300,000 increases the cost by 7.84%, 8.13%, 10.37%, and 14.27% under the 0–48, 12–36, 24–36, and 36–48 time windows, respectively. The largest increase occurs

under the 36–48 time window, indicating that the additional procurement cost of tighter carbon restrictions varies with time-window requirements. Table 7 further shows that maximum scenario emissions under the 12–36 time window decrease from 452,610.64 to 300,000. The increase in procurement cost and the decrease in emissions jointly reflect the cost of meeting stricter carbon restrictions.

As shown in Figure 8(b), expected emergency outsourcing volume generally decreases as the carbon cap is tightened. Table 7 shows that when the cap decreases from 500,000 to 300,000 under the 12–36 time window, the expected emergency outsourcing volume falls from 2615.00 to 894.50, and the fortification configuration changes from one bid at level 3 to two bids at level 2 and two bids at level 3. The decline in emergency outsourcing volume is accompanied by a wider deployment of fortification, indicating that tighter carbon restrictions affect both postdisruption transportation arrangements and predisruption protection decisions.

In summary, 4PLs should jointly consider the carbon-emission cap and time-window requirements when designing procurement plans. Under the 36–48 time window, where emission reductions incur a larger cost increase, 4PLs should assess the additional procurement expenditure required to meet the carbon cap in advance, jointly configure fortification and capacity reservation, and arrange postdisruption transportation allocation and emergency outsourcing accordingly. Resilience investment should be guided by total procurement cost, emission compliance, and demand fulfillment rather than simply increasing the number of fortified bids or the amount of reserved capacity.

5.4. Strategy comparison

Comparative experiments are conducted to evaluate the capacity reservation and fortification strategies. The protective investment budget $C_{\max}$ is set to 1000, 5000, 10,000, 30,000, and 50,000; the unit emergency outsourcing cost e is set to 100, 150, 300, 500, and 1000; and four soft time-window settings, 0–48, 12–36, 24–36, and 36–48, are considered. The value of capacity reservation or fortification is quantified by comparing the total procurement cost and total emergency outsourcing cost between cases with and without the corresponding strategy, thereby identifying the cost effects of each strategy and the conditions under which it is effective. The results are presented in Figures 9 and 10 and the corresponding tables.

5.4.1. Effects of the capacity reservation strategy

To evaluate the effects of capacity reservation on costs, comparative experiments are conducted under the parameter settings specified in Section 5.4, and the value of the strategy is quantified by comparing the results obtained with and without capacity reservation. Let G denote the difference in total procurement costs between cases without and with capacity reservation, and let Y denote the corresponding differences in total emergency outsourcing costs. Positive values of G and Y indicate cost reductions achieved by capacity reservation, whereas negative values indicate cost increases; larger absolute values represent larger changes. The detailed results are reported in Table 8 and Figure 9.

Table 8. Cost differences between cases with and without capacity reservation.

T	e	Measure	$C_{\max}$				
			1000	5000	10,000	30,000	50,000
0–48	e = 100	G	4988.71	9083.80	12,419.65	28,002.16	28,040.00
0–48	e = 100	Y	-7180.53	17,360.00	-18,756.86	6772.63	5820.00
0–48	e = 150	G	7393.74	12,868.69	14,232.66	46,344.51	47,206.57
0–48	e = 150	Y	12,229.26	12,648.50	1320.19	43,631.23	56,899.52
0–48	e = 300	G	42,104.21	60,593.14	68,460.84	86,569.15	92,297.00
0–48	e = 300	Y	67,038.86	110,495.67	108,513.53	71,109.83	78,300.00
0–48	e = 500	G	63,255.35	87,689.17	136,584.94	119,974.13	130,697.00
0–48	e = 500	Y	8675.00	71,195.84	92,210.65	93,666.67	114,500.00
0–48	e = 1000	G	133,652.56	181,073.68	239,948.43	236,459.90	252,067.60
0–48	e = 1000	Y	137,811.90	183,465.65	258,046.13	251,333.33	256,000.00
12–36	e = 100	G	5130.44	9575.80	16,746.89	32,278.00	32,278.00
12–36	e = 100	Y	29,777.78	17,360.00	-12,334.26	-33,300.00	-33,300.00
12–36	e = 150	G	7319.19	14,547.89	16,221.36	51,986.51	52,676.08
12–36	e = 150	Y	13,154.69	-5337.42	7911.84	45,131.23	38,317.31
12–36	e = 300	G	39,348.40	55,172.23	67,208.55	92,031.82	99,190.00
12–36	e = 300	Y	75,330.00	108,641.20	108,357.64	61,500.00	83,700.00
12–36	e = 500	G	65,410.35	85,326.95	139,140.94	125,367.35	133,833.00
12–36	e = 500	Y	8675.00	49,937.65	92,210.65	93,000.00	114,500.00
12–36	e = 1000	G	134,684.56	178,811.68	238,203.24	239,449.90	251,855.60
12–36	e = 1000	Y	137,811.90	183,465.65	245,135.41	251,333.33	256,000.00
24–36	e = 100	G	5607.84	10,253.31	19,973.82	38,105.00	38,105.00
24–36	e = 100	Y	-23,047.37	20,917.24	33,552.39	98,700.00	98,700.00
24–36	e = 150	G	12,044.84	25,605.32	23,278.05	60,515.00	60,593.80
24–36	e = 150	Y	24,134.21	-7429.45	38,360.67	73,350.00	82,567.31
24–36	e = 300	G	39,747.52	62,346.10	72,450.49	101,459.00	111,791.00
24–36	e = 300	Y	74,786.36	69,044.38	106,411.96	27,000.00	60,600.00
24–36	e = 500	G	70,394.15	89,745.64	148,655.97	140,868.79	148,813.00
24–36	e = 500	Y	46,558.93	46,111.55	191,306.61	93,000.00	89,750.00
24–36	e = 1000	G	130,795.56	177,878.75	235,798.44	248,587.28	268,488.00
24–36	e = 1000	Y	137,811.90	173,309.39	230,466.30	228,000.00	229,000.00
36–48	e = 100	G	5512.84	10,665.31	20,033.62	39,276.00	39,276.00
36–48	e = 100	Y	53,052.63	78,717.24	140,862.50	203,800.00	203,800.00
36–48	e = 150	G	15,157.00	37,032.85	44,760.26	92,653.88	96,900.00
36–48	e = 150	Y	17,265.79	39,196.55	-37,082.43	132,046.88	133,650.00
36–48	e = 300	G	55,858.18	82,547.04	111,221.48	126,148.00	136,930.22
36–48	e = 300	Y	92,182.11	64,759.26	97,313.36	22,800.00	29,726.92
36–48	e = 500	G	65,689.15	113,990.05	177,316.08	159,601.13	172,264.00
36–48	e = 500	Y	46,558.93	66,900.84	184,943.95	73,500.00	45,000.00
36–48	e = 1000	G	120,136.33	211,972.76	250,681.84	261,857.00	298,004.00
36–48	e = 1000	Y	89,700.00	248,838.44	174,426.25	256,000.00	261,000.00

As shown in Figure 9(a), the total procurement-cost difference G generally increases with the protective investment budget $C_{\max}$, indicating that the cost-saving effect of capacity reservation becomes more pronounced as the available budget increases. At the same budget level, G is generally larger under tighter time-window settings, suggesting that capacity reservation provides greater cost-saving benefits when timeliness requirements are more stringent. Moreover, the increase in G becomes more pronounced at higher values of e, indicating that larger total-cost reductions are obtained from capacity reservation when emergency outsourcing is more costly.

Figure 9(b) indicates that the effect of capacity reservation on emergency outsourcing cost varies across the tested parameter settings. Although capacity reservation reduces the emergency outsourcing cost in most cases, negative values of Y occur under several combinations of budget, outsourcing cost, and soft time-window settings, reflecting interactions among reserved capacity, task reallocation, and emergency outsourcing decisions.

Overall, capacity reservation reduces total procurement cost across all tested settings, with larger reductions generally observed at higher unit emergency outsourcing costs and under tighter time

windows. The effect on emergency outsourcing cost varies because reserved capacity can alter transportation task allocation among the winning 3PLs. These results indicate that capacity reservation primarily provides flexible capacity support after disruptions.

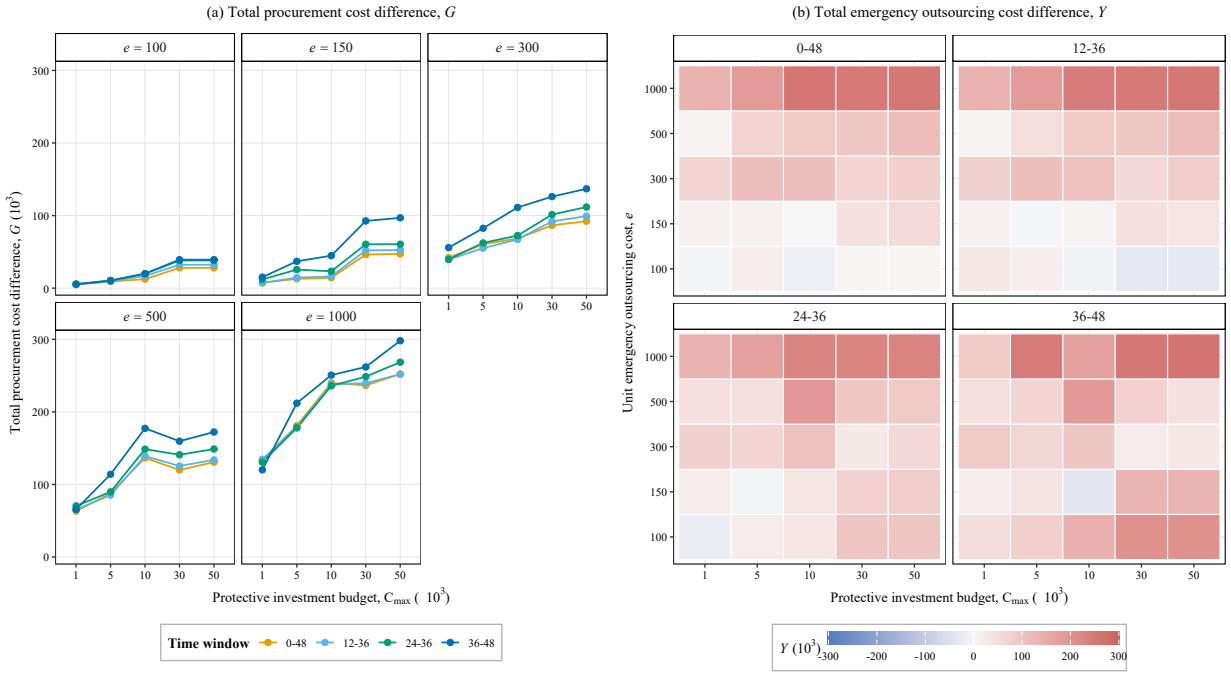


Figure 9. Effects of capacity reservation on total procurement and emergency outsourcing costs.

5.4.2. Effects of the multilevel fortification strategy

To evaluate the effects of multilevel fortification on costs, comparative experiments are conducted under the parameter settings specified in Section 5.4 by comparing the results obtained with and without fortification. Let S denote the difference in total procurement cost between cases without and with multilevel fortification, and let M denote the corresponding difference in total emergency outsourcing cost. Positive values of S and M indicate cost reductions achieved by multilevel fortification, whereas negative values indicate cost increases; larger absolute values represent larger changes. Results are reported in Table 9 and Figure 10.

Table 9. Cost differences between cases with and without multilevel fortification.

T	e	Measure	$C_{\max}$			
			5000	10,000	30,000	50,000
0–48	e = 100	S	2726.30	8753.13	17,530.16	17,568.00
0–48	e = 100	M	-17,277.84	-26,169.64	952.63	0.00
0–48	e = 150	S	0.00	4504.63	27,285.49	28,147.55
0–48	e = 150	M	0.00	2880.19	9137.23	22,405.52
0–48	e = 300	S	0.00	13,666.26	25,080.29	30,808.14
0–48	e = 300	M	0.00	17,494.17	-4966.42	2223.75
0–48	e = 500	S	0.00	20,156.96	29,330.73	40,053.60
0–48	e = 500	M	0.00	11,135.40	29,516.67	50,350.00
0–48	e = 1000	S	0.00	0.00	30,779.90	46,387.60
0–48	e = 1000	M	0.00	0.00	11,513.33	16,180.00

Table 9. (continued)

T	e	Measure	C_{max}			
			5000	10,000	30,000	50,000
12–36	e = 100	S	2158.81	7751.21	18,312.00	18,312.00
12–36	e = 100	M	-19,277.93	-42,494.58	0.00	0.00
12–36	e = 150	S	0.00	4444.74	29,884.49	30,574.06
12–36	e = 150	M	0.00	31,576.50	9137.23	2323.31
12–36	e = 300	S	0.00	12,961.32	27,469.95	34,628.13
12–36	e = 300	M	0.00	14,994.07	-10,020.00	12,180.00
12–36	e = 500	S	0.00	22,229.96	32,757.53	41,223.18
12–36	e = 500	M	0.00	11,135.40	29,075.00	50,575.00
12–36	e = 1000	S	0.00	2604.76	29,978.90	42,384.60
12–36	e = 1000	M	0.00	-5187.03	11,513.33	16,180.00
24–36	e = 100	S	742.08	7522.57	18,733.00	18,733.00
24–36	e = 100	M	-26,032.76	19,395.00	0.00	0.00
24–36	e = 150	S	0.00	4417.82	31,407.80	31,486.60
24–36	e = 150	M	0.00	-504.33	-2805.00	6412.31
24–36	e = 300	S	0.00	16,264.18	31,341.70	41,673.70
24–36	e = 300	M	0.00	29,794.37	-26,475.00	7125.00
24–36	e = 500	S	0.00	25,732.62	43,467.53	51,411.73
24–36	e = 500	M	0.00	23,087.12	43,200.00	39,950.00
24–36	e = 1000	S	0.00	14,388.85	57,062.08	76,962.80
24–36	e = 1000	M	0.00	1763.32	-10,800.00	-9800.00
36–48	e = 100	S	1921.45	9186.38	20,743.00	20,743.00
36–48	e = 100	M	-38,094.76	-21,461.03	-123,300.00	-123,300.00
36–48	e = 150	S	0.00	0.00	29,793.88	34,040.00
36–48	e = 150	M	0.00	0.00	87,646.88	89,250.00
36–48	e = 300	S	0.00	19,148.17	31,877.40	42,659.62
36–48	e = 300	M	0.00	20,695.77	-34,905.00	-27,978.08
36–48	e = 500	S	0.00	32,516.08	31,039.53	43,702.40
36–48	e = 500	M	0.00	32,313.30	41,400.00	12,900.00
36–48	e = 1000	S	0.00	28,484.45	57,538.50	93,685.50
36–48	e = 1000	M	0.00	-16,309.16	28,700.00	33,700.00

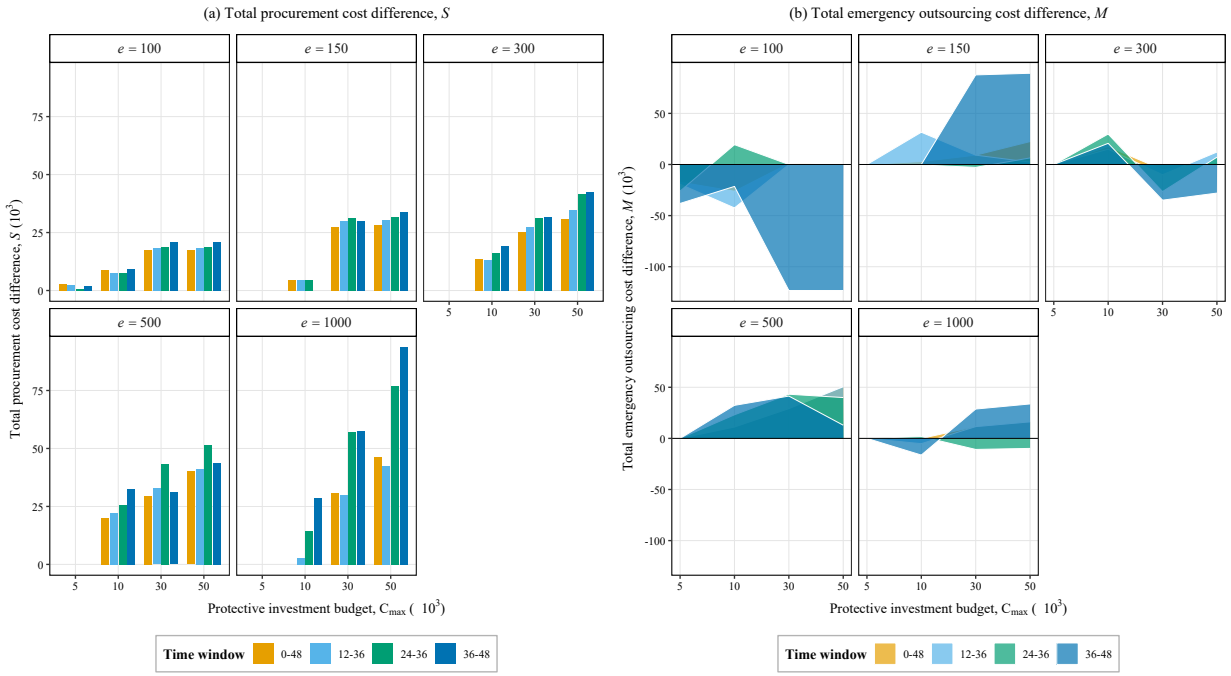


Figure 10. Effects of multilevel fortification on total procurement and emergency outsourcing costs.

Figure 10(a) indicates that the total procurement cost difference S generally increases with the protective investment budget $C_{\max}$, with a more pronounced increase under the 36–48 time window setting. The larger value of S under $T = [36, 48]$ indicates that fortification is more effective in reducing disruption-induced additional costs when timeliness requirements are stringent or when flexibility for transportation adjustment is limited. When the unit emergency outsourcing cost e is low, S increases relatively slowly; as e rises, however, S increases markedly, indicating that multilevel fortification produces larger total-cost reductions when emergency outsourcing is more costly.

The effect of fortification on emergency outsourcing cost varies across the tested settings. Although higher protective investment enables stronger fortification, negative values of M remain under some parameter combinations, indicating that changes in task allocation can produce higher emergency outsourcing costs in these cases. By contrast, S remains non-negative across the tested settings, supporting the cost-saving value of fortification in terms of total procurement cost.

Overall, S is zero or positive across all tested settings, indicating that multilevel fortification maintains or reduces total procurement cost in the tested cases. Larger total-cost reductions are generally observed when the protective investment budget is higher, emergency outsourcing is more costly, and time windows are tighter. The effect on emergency outsourcing cost varies because changes in retained transportation capacity may alter the resulting task-allocation structure. These results support the role of multilevel fortification as a predisruption capacity-protection strategy.

5.4.3. Cost comparison of resilience strategies

To further assess the hybrid resilience strategy, a baseline without fortification or capacity reservation is introduced (with emergency outsourcing retained) and compared with fortification only, capacity reservation only, and the hybrid strategy. All four strategies use the same demand, bundle bids, and disruption scenarios. The protective investment budget is set to 50,000, the time window to 12–36, and the unit emergency outsourcing cost to 100, 500, and 1000. Table 10 and Figure 11 report total procurement cost (TC) and expected emergency outsourcing cost (W_1) for each strategy.

Table 10. Total procurement cost and expected emergency outsourcing cost under different resilience strategies.

e	Measure	Baseline	Fortification only	Capacity reservation only	Hybrid strategy
100	TC	1,585,092.00	1,561,924.00	1,547,958.00	1,529,646.00
	W_1	332,900.00	228,200.00	261,500.00	261,500.00
500	TC	1,983,279.60	1,800,554.00	1,707,944.18	1,666,721.00
	W_1	275,625.00	128,000.00	64,075.00	13,500.00
1000	TC	2,251,714.87	1,928,554.00	1,719,083.00	1,676,698.40
	W_1	526,866.67	256,000.00	16,180.00	0.00

As shown in Table 10 and Figure 11(a), the hybrid strategy reduces total procurement cost by 3.50%, 15.96%, and 25.54% relative to the baseline in the three settings, respectively, and achieves lower total procurement costs than either individual strategy. Table 10 and Figure 11(b) show that at $e = 100$, fortification only incurs a lower emergency outsourcing cost than the hybrid strategy, but the

hybrid strategy still achieves the lowest total procurement cost, indicating that emergency outsourcing expenditure alone is insufficient to assess overall strategy performance. As e increases to 500 and 1000, emergency outsourcing cost under the hybrid strategy falls to 13,500 and zero, respectively, but total-cost reductions relative to the baseline increase to 15.96% and 25.54%, indicating a more pronounced cost advantage for the hybrid strategy when emergency outsourcing is expensive. For 4PLs, resilience strategy selection should account for predisruption investment and postdisruption fulfillment costs; when emergency outsourcing prices are high, combining fortification and capacity reservation can help control overall procurement cost.

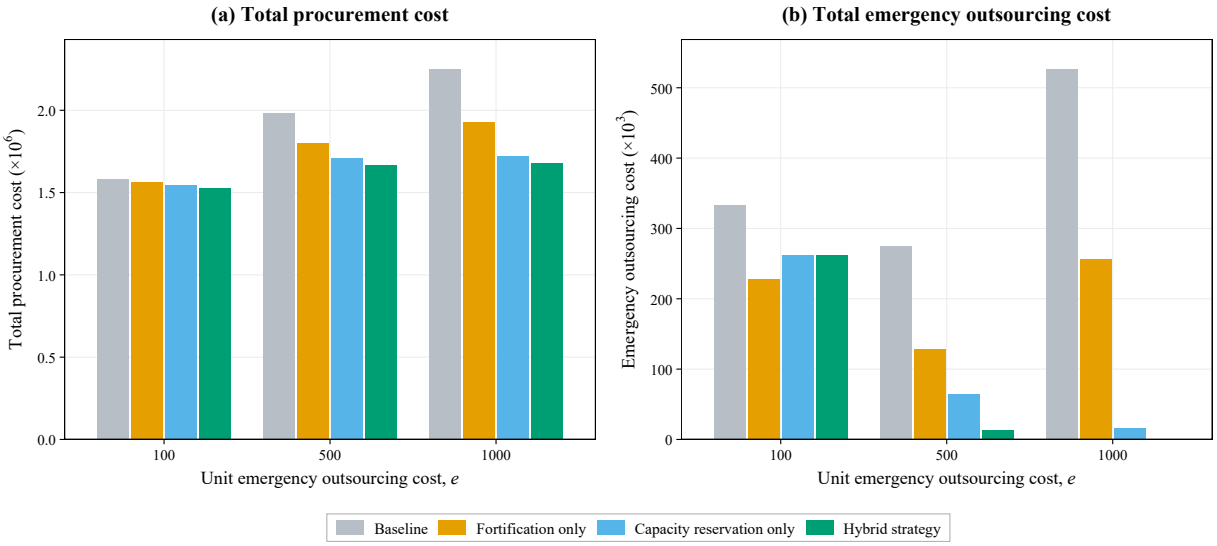


Figure 11. Comparison of total procurement cost and expected emergency outsourcing cost under different resilience strategies.

5.5. Managerial insights

The numerical results and strategy comparisons yield the following managerial insights for 4PLs configuring the hybrid resilience strategy.

First, differentiated disruption-response strategies should be adopted according to time window stringency and the unit emergency outsourcing cost. When time windows are tight, and the unit emergency outsourcing cost remains acceptable, emergency outsourcing can rapidly supplement transportation capacity after disruptions and help maintain timeliness while reducing tardiness penalties. However, when emergency outsourcing becomes costly, excessive reliance on postdisruption outsourcing can substantially increase the total procurement cost. For this reason, when a high unit emergency outsourcing cost coincides with stringent timeliness requirements, capacity reservation and fortification should be configured in advance to reduce reliance on costly emergency outsourcing after disruptions. Accordingly, when configuring disruption-response strategies, 4PLs should jointly assess their implications for timeliness, emergency outsourcing cost, and compliance with the carbon-emission cap.

Second, capacity reservation is more suitable for strengthening postdisruption response capability. The experimental results show that capacity reservation consistently reduces the total procurement

cost, whereas the effect on emergency outsourcing cost varies across some parameter settings. When sufficient budget is available, and the unit emergency outsourcing cost is high, reserved capacity can replace part of the emergency outsourcing requirement and reduce postdisruption response costs, although changes in task allocation may occasionally increase emergency outsourcing cost. Under limited budgets, however, only a small amount of capacity can be reserved, and the resulting cost-saving effect may be limited. Accordingly, 4PLs should prioritize capacity reservation for critical 3PL bundle bids rather than spreading limited investment across too many alternatives.

Third, multilevel fortification is more suitable for the predisruption protection of critical 3PL bundle bids. Compared with capacity reservation, fortification places greater emphasis on preserving the transportation capacity associated with selected 3PL bundle bids before disruptions occur. The experimental results show that the cost-saving effect of fortification is more pronounced when the protective investment budget is sufficient, the unit emergency outsourcing cost is high, and timeliness requirements are stringent. In practice, fortification should be prioritized for bundle bids with high disruption probabilities, large potential capacity losses, or critical roles in maintaining timeliness.

Fourth, under the parameter settings of the case study, increasing the protective investment budget from 10,000 to 30,000 yields substantial cost reductions, with diminishing marginal savings at higher budget levels. When determining the protective investment budget, 4PLs should identify a cost-effective investment range based on the unit emergency outsourcing cost and time window stringency rather than simply pursuing a higher budget. As a complementary managerial measure outside the modeled decisions, 4PLs may expand the pool of reliable candidate 3PLs to improve alternative service capacity and decision flexibility under disruptions.

Overall, these insights support 4PLs in coordinating multiple 3PL resources and developing LSSP plans that balance greenness, timeliness, and resilience under disruption risk.

6. Conclusions

This study investigates a WDP for LSSP auctions under stochastic disruption risk and soft time windows, integrating greenness, timeliness, and resilience within a unified decision framework that incorporates a carbon-emission cap. A two-stage stochastic WD model is formulated to minimize the 4PL's expected total procurement cost. Disruption-induced changes in available 3PL capacity, carbon-emission control, soft time-window penalties, emergency outsourcing, capacity reservation, and multilevel fortification are incorporated into a unified decision framework to characterize the interactions among 3PL selection, transportation task allocation, protective investment, and timeliness under disruptions. To address the computational difficulties arising from the rapid growth in model size as the number of disruption scenarios increases, an SR-SSDDLR hybrid algorithm is developed. SR is employed to construct a feasible upper bound, and the improved SSDDLR method is used to obtain an effective lower bound.

The numerical results for the African container shipping case show that for instances involving 29 shipping routes, 42 candidate 3PLs, and 1024 disruption scenarios, SR-SSDDLR obtains feasible solutions in 53.08–184.52 s, with gaps of 0.44%–1.89%. Direct CPLEX solution in the 64GB environment yields higher-cost feasible solutions under a common 3600 s time limit. The parameter analysis indicates that the unit emergency outsourcing cost, protective investment budget, and soft time-window settings affect the 4PL's configuration of the hybrid resilience strategy. Under the

case-study settings, substantial cost reductions are achieved as the budget increases to 30,000, with diminishing marginal savings at higher budget levels. Strategy comparisons indicate that capacity reservation and multilevel fortification reduce total procurement cost under appropriate conditions, but the effects of both strategies on emergency outsourcing cost vary with the tested parameter settings. Capacity reservation primarily supports postdisruption capacity supplementation, whereas multilevel fortification is better-suited to protecting critical 3PL bundle bids before disruptions occur.

Overall, stochastic disruption risk, carbon-emission control, soft time-window penalties, multi-3PL sourcing, and the hybrid resilience strategy are integrated within a unified WDP framework. Computational efficiency for problems involving large numbers of disruption scenarios is improved by the proposed SR-SSDDLR algorithm, and coordinated 4PL decisions on 3PL selection, protective investment, and cost–timeliness trade-offs are supported by the integrated modeling and solution framework in liner-shipping environments subject to disruption risk. The proposed framework supports 4PLs in coordinating multiple 3PL resources and developing LSSP plans that balance greenness, timeliness, and resilience under disruptions.

Future research may extend the present study in several directions. First, dynamic demand in a multiperiod setting and rolling-horizon decision-making mechanisms can be introduced to capture demand fluctuations and the evolution of disruptions in LSSP. At each decision point, updated demand forecasts [42] could inform procurement decisions, and feedback-based compensation [43] could help refine estimates of available capacity. Second, strategic bidding by 3PLs, information asymmetry, and service reliability learning mechanisms can be considered to improve the model's representation of real-world auction environments. The reinforcement learning approach used by Li et al. [44] for sensor selection with unknown noise covariances could also inform future exploration of adaptive provider-selection when service-performance information is incomplete. Third, correlated disruptions, the propagation of port congestion, interdependencies within liner-shipping route networks, and multimodal-transportation coordination can be incorporated to improve risk characterization and broaden model applicability. In addition, route-specific emission and fuel-consumption data and more flexible carbon-management mechanisms can be examined in future research.

Author contributions

Mingkun Yu: Methodology, Software, Formal analysis, Data curation, Visualization, Writing–original draft. **Liyan Wang:** Conceptualization, Validation, Supervision, Writing–review & editing. **Mingqiang Yin:** Conceptualization, Methodology, Software, Formal analysis, Validation, Writing–review & editing, Funding acquisition. **Linlin Kong:** Data curation, Validation, Visualization. **Guihua Bo:** Resources, Validation. **Xiaohu Qian:** Validation, Supervision.

Use of Generative-AI tools declaration

During the preparation of this manuscript, the authors used ChatGPT (OpenAI) solely for English translation and language polishing. The authors reviewed and revised all AI-assisted language edits and take full responsibility for the final content of the manuscript.

Acknowledgments

This work was supported by the China Postdoctoral Science Foundation (2025MD784090); the Social Science Foundation of Liaoning Province (L24CGL031); the Foundation of the Educational Department of Liaoning Province (LJ212610148020; LJ222610148008; LJ212610148006; LJ222610148012); the "Xingliao Talent Program" Leading Talents Project of Liaoning Province (XLYC2402025); the National Local Joint Engineering Laboratory Project for Optimization of Petrochemical Process Operations and Energy Saving Technology of the Education Department of Liaoning Province (LJ232510148001); and the Foundation of Talent Scientific Research Fund of LNPU (2023XJJL-004).

Conflict of interest

All authors declare no conflicts of interest in this paper.

References

1. United Nations Conference on Trade and Development (UNCTAD), *Review of maritime transport 2024: Navigating maritime chokepoints*, UNCTAD/RMT/2024, United Nations, Geneva, 2024. https://doi.org/10.18356/9789211065923
2. Y. Tao, E. P. Chew, L. H. Lee, Y. Shi, A column generation approach for the route planning problem in fourth party logistics, *J. Oper. Res. Soc.,* **68** (2017), 165–181. https://doi.org/10.1057/s41274-016-0024-3
3. X. Qian, M. Yin, F. T. S. Chan, K. Yue, Winner determination with sustainable-flexible considerations under demand uncertainty in transportation service procurement auctions, *Netw. Spat. Econ.,* **23** (2023), 953–984. https://doi.org/10.1007/s11067-023-09599-8
4. Y. Zhou, M. Yin, Q. Liu, X. Qian, D. Jin, X. Lang, Optimizing winner determination for sustainability and timeliness in fresh agricultural product logistics service procurement auctions: insights from a fourth-party logistics perspective, *Front. Sustain. Food Syst.,* **9** (2025), 1585053. https://doi.org/10.3389/fsufs.2025.1585053
5. N. K. Tran, H. Haralambides, T. Notteboom, K. Cullinane, The costs of maritime supply chain disruptions: The case of the Suez Canal blockage by the 'Ever Given' megaship, *Int. J. Prod. Econ.,* **279** (2025), 109464. https://doi.org/10.1016/j.ijpe.2024.109464
6. W. Y. Yap, D. Yang, Geopolitical tension and shipping network disruption: Analysis of the Red Sea crisis on container port calls, *J. Transp. Geogr.,* **121** (2024), 104004. https://doi.org/10.1016/j.jtrangeo.2024.104004
7. United Nations Conference on Trade and Development (UNCTAD), *Strait of Hormuz disruptions: Implications for global trade and development*, UNCTAD/OSG/TT/INF/2026/1, United Nations, Geneva, 2026.
8. M. Salani, M. Battarra, The opportunity cost of time window violations, *EURO J. Transp. Logist.,* **7** (2018), 343–361. https://doi.org/10.1007/s13676-018-0121-3

9. S. El Noshokaty, Shipping optimization systems (SOS) for tramp: stochastic cargo soft time windows, *J. Shipp. Trade,* **6** (2021), 17. https://doi.org/10.1186/s41072-021-00097-z
10. Y. Sheffi, Combinatorial auctions in the procurement of transportation services, *Interfaces,* **34** (2004), 245–252. https://doi.org/10.1287/inte.1040.0075
11. M. R. Hasan, A. Elomri, C. Triki, Combinatorial-based auction for the transportation procurement: An optimization-oriented review, *IEEE Access,* **11** (2023), 60191–60210. https://doi.org/10.1109/ACCESS.2023.3284310
12. Z. Ma, R. H. Kwon, C. G. Lee, A stochastic programming winner determination model for truckload procurement under shipment uncertainty, *Transp. Res. Part E Logist. Transp. Rev.,* **46** (2010), 49–60. https://doi.org/10.1016/j.tre.2009.02.002
13. N. Remli, M. Rekik, A robust winner determination problem for combinatorial transportation auctions under uncertain shipment volumes, *Transp. Res. Part C Emerg. Technol.,* **35** (2013), 204–217. https://doi.org/10.1016/j.trc.2013.07.006
14. B. Zhang, T. Yao, T. L. Friesz, Y. Sun, A tractable two-stage robust winner determination model for truckload service procurement via combinatorial auctions, *Transp. Res. Part B Methodol.,* **78** (2015), 16–31. https://doi.org/10.1016/j.trb.2015.03.019
15. N. Remli, A. Amrouss, I. El Hallaoui, M. Rekik, A robust optimization approach for the winner determination problem with uncertainty on shipment volumes and carriers' capacity, *Transp. Res. Part B Methodol.,* **123** (2019), 127–148. https://doi.org/10.1016/j.trb.2019.03.017
16. M. Safari, A. Dolati, On the winner determination problem with uncertain bids' prices, *Iran. J. Sci. Technol. Trans. Sci.,* **46** (2022), 1265–1273. https://doi.org/10.1007/s40995-022-01340-3
17. N. Li, Y. Zhang, S. Tiwari, G. Kou, Winner determination problem with purchase budget for transportation procurement under uncertain shipment volume, *Transp. Res. Part E Logist. Transp. Rev.,* **176** (2023), 103182. https://doi.org/10.1016/j.tre.2023.103182
18. X. Qian, M. Yin, X. Li, Q. Zhang, Two-stage stochastic nonlinear winner determination for logistics service procurement auctions under quantity discounts, *J. Ind. Manag. Optim.,* **19** (2023), 7072–7089. https://doi.org/10.3934/jimo.2022252
19. Y. Fu, K. Z. Gao, L. Wang, M. Huang, Y. C. Liang, H. Y. Dong, Scheduling stochastic distributed flexible job shops using an multi-objective evolutionary algorithm with simulation evaluation, *Int. J. Prod. Res.,* **63** (2025), 86–103. https://doi.org/10.1080/00207543.2024.2356628
20. P. R. Kleindorfer, G. H. Saad, Managing disruption risks in supply chains, *Prod. Oper. Manag.,* **14** (2005), 53–68. https://doi.org/10.1111/j.1937-5956.2005.tb00009.x
21. X. Qian, F. T. S. Chan, M. Yin, Q. Zhang, M. Huang, X. Fu, A two-stage stochastic winner determination model integrating a hybrid mitigation strategy for transportation service procurement auctions, *Comput. Ind. Eng.,* **149** (2020), 106703. https://doi.org/10.1016/j.cie.2020.106703
22. M. Yin, X. Qian, M. Huang, Q. Zhang, Winner determination for logistics service procurement auctions under disruption risks and quantity discounts, *Eng. Appl. Artif. Intell.,* **105** (2021), 104424. https://doi.org/10.1016/j.engappai.2021.104424

23. W. Zhang, K. Wang, A. Jacquillat, S. Wang, Optimized scenario reduction: Solving large-scale stochastic programs with quality guarantees, *INFORMS J. Comput.,* **35** (2023), 886–908. https://doi.org/10.1287/ijoc.2023.1295
24. D. Bertsimas, N. Mundru, Optimization-based scenario reduction for data-driven two-stage stochastic optimization, *Oper. Res.,* **71** (2022), 1343–1361. https://doi.org/10.1287/opre.2022.2265
25. M. Yin, H. Wang, Q. Liu, X. Qian, H. Zhang, X. Lang, A sampling-based winner determination model and algorithm for logistics service procurement auctions under double uncertainty, *Sci. Rep.,* **15** (2025), 12054. https://doi.org/10.1038/s41598-025-94748-x
26. A. Jabbarzadeh, B. Fahimnia, J. B. Sheu, H. Shahmoradi Moghadam, Designing a supply chain resilient to major disruptions and supply/demand interruptions, *Transp. Res. Part B Methodol.,* **94** (2016), 121–149. https://doi.org/10.1016/j.trb.2016.09.004
27. T. Sawik, Disruption mitigation and recovery in supply chains using portfolio approach, *Omega,* **84** (2019), 232–248. https://doi.org/10.1016/j.omega.2018.05.006
28. X. Qian, M. Yin, F. T. S. Chan, J. Zhang, M. Huang, Sustainable–responsive winner determination for transportation service procurement auctions under accidental disruptions, *J. Clean. Prod.,* **320** (2021), 128833. https://doi.org/10.1016/j.jclepro.2021.128833
29. Y. Zhou, D. Dong, M. Yin, Q. Liu, X. Qian, X. Li, Transforming resilient fourth-party logistics networks: An innovative hybrid mitigation strategy for disruption risks, *J. Ind. Manag. Optim.,* **21** (2025), 7132–7160. https://doi.org/10.3934/jimo.2025162
30. M. Yin, Y. Zhou, X. Qian, Q. Liu, X. Guo, Optimizing multi-period green electric vehicle battery recycling network: Integrating winner determination within a 4PL framework, *IEEE Trans. Eng. Manag.,* **73** (2026), 1769–1783. https://doi.org/10.1109/TEM.2026.3658193
31. X. Wang, Q. Liu, M. Yin, Transforming electric vehicle battery recycling network with integrated winner determination for enhanced resilience, *Comput. Chem. Eng.,* **208** (2026), 109561. https://doi.org/10.1016/j.compchemeng.2026.109561
32. Z. Wang, Z. Zhang, M. Yin, N. Yuan, X. Qian, X. Li, 4PL-Driven optimization of electric vehicle battery recycling networks: enhancing greenness, timeliness and resilience against disruptions, *Waste Manag.,* **222** (2026), 115650. https://doi.org/10.1016/j.wasman.2026.115650
33. Q. Hu, Z. Zhang, A. Lim, Transportation service procurement problem with transit time, *Transp. Res. Part B Methodol.,* **86** (2016), 19–36. https://doi.org/10.1016/j.trb.2016.01.007
34. C. Y. Lee, S. Shu, Z. Xu, Optimal global liner service procurement by utilizing liner service schedules, *Prod. Oper. Manag.,* **30** (2021), 703–714. https://doi.org/10.1111/poms.13311
35. F. Yang, F. J. Hwang, Y. H. Huang, A two-stage method for the shipper lane selection problem with time windows in transportation service procurement, *Int. Trans. Oper. Res.,* **31** (2024), 2209–2230. https://doi.org/10.1111/itor.13243
36. R. Jothi Basu, R. Bai, PL. K. Palaniappan, A strategic approach to improve sustainability in transportation service procurement, *Transp. Res. Part E Logist. Transp. Rev.,* **74** (2015), 152–168. https://doi.org/10.1016/j.tre.2014.10.015

37. C. Triki, M. R. Hasan, A. Elomri, Solving the winner determination problem with discounted bids in transportation auctions, *Ann. Oper. Res.,* **351** (2025), 35–58. https://doi.org/10.1007/s10479-023-05457-5

38. H. C. Lau, B. Li, Solving the winner determination problem for online B2B transportation matching platforms, *Transp. Res. Part E Logist. Transp. Rev.,* **150** (2021), 102324. https://doi.org/10.1016/j.tre.2021.102324

39. L. V. Snyder, M. S. Daskin, Models for reliable supply chain network design, in *Critical Infrastructure: Reliability and Vulnerability* (eds. A. T. Murray and T. H. Grubesic), Springer, Berlin, Heidelberg, 2007, 257–289. https://doi.org/10.1007/978-3-540-68056-7_13

40. M. Yin, M. Huang, D. Wang, S. C. Fang, X. Qian, X. Wang, Multi-period fourth-party logistics network design with the temporary outsourcing service under demand uncertainty, *Comput. Oper. Res.,* **164** (2024), 106564. https://doi.org/10.1016/j.cor.2024.106564

41. B. D. Brouer, J. F. Alvarez, C. E. M. Plum, D. Pisinger, M. M. Sigurd, A base integer programming model and benchmark suite for liner-shipping network design, *Transp. Sci.,* **48** (2013), 281–312. https://doi.org/10.1287/trsc.2013.0471

42. M. Yin, Z. Han, X. Qian, G. Bo, X. Li, From predictive accuracy to prescriptive value: A data-driven framework for sustainable multi-period electric vehicle battery recycling networks, *J. Clean. Prod.,* **574** (2026), 149022. https://doi.org/10.1016/j.jclepro.2026.149022

43. B. Peng, H. Y. Shi, T. Y. Chai, C. L. Su, P. Li, Improved predictive functional control based on unmodeled dynamics compensation for ethylene cracking furnace, *IEEE Trans. Ind. Electron.*, (2026). https://doi.org/10.1109/TIE.2026.3695191

44. J. Li, X. Wang, X. Meng, F. L. Lewis, Optimal sensor selection of linear quadratic regulation with unknown sensor noise covariances, *IEEE/CAA J. Autom. Sinica,* **13** (2026), 1747–1754. https://doi.org/10.1109/JAS.2025.125915



AIMS Press

© 2026 the Author(s), licensee AIMS Press. This is an open access article distributed under the terms of the Creative Commons Attribution License (https://creativecommons.org/licenses/by/4.0)